

1981

# Some chemical and mineralogical aspects of plutonic rocks from the North Arm Mountain Massif, Bay Of Islands Ophiolite, Newfoundland

Jerry W. Sullivan

*University at Albany, State University of New York*

Follow this and additional works at: [http://scholarsarchive.library.albany.edu/  
cas\\_daes\\_geology\\_etd](http://scholarsarchive.library.albany.edu/cas_daes_geology_etd)

 Part of the [Geochemistry Commons](#), [Geology Commons](#), and the [Sedimentology Commons](#)

---

## Recommended Citation

Sullivan, Jerry W., "Some chemical and mineralogical aspects of plutonic rocks from the North Arm Mountain Massif, Bay Of Islands Ophiolite, Newfoundland" (1981). *Geology Theses and Dissertations*. 90.  
[http://scholarsarchive.library.albany.edu/cas\\_daes\\_geology\\_etd/90](http://scholarsarchive.library.albany.edu/cas_daes_geology_etd/90)

This Thesis is brought to you for free and open access by the Atmospheric and Environmental Sciences at Scholars Archive. It has been accepted for inclusion in Geology Theses and Dissertations by an authorized administrator of Scholars Archive. For more information, please contact [scholarsarchive@albany.edu](mailto:scholarsarchive@albany.edu).

SOME CHEMICAL AND MINERALOGICAL ASPECTS OF PLUTONIC ROCKS  
FROM THE NORTH ARM MOUNTAIN MASSIF,  
BAY OF ISLANDS OPHIOLITE,  
NEWFOUNDLAND

A thesis presented to the Faculty of the  
State University of New York at Albany  
in partial fulfillment of the requirements for the degree of  
Master of Science

College of Science and Mathematics  
Department of Geological Sciences

Jerry W. Sullivan

1981

SOME CHEMICAL AND MINERALOGICAL ASPECTS OF PLUTONIC ROCKS  
FROM THE NORTH ARM MOUNTAIN MASSIF,  
BAY OF ISLANDS OPHIOLITE,  
NEWFOUNDLAND

Abstract of  
A thesis presented to the Faculty of the  
State University of New York at Albany  
in partial fulfillment of the requirements for the degree of  
Master of Science

College of Science and Mathematics  
Department of Geological Sciences

Jerry W. Sullivan

1981

954578 0

UNIVERSITY LIBRARY

## ABSTRACT

Whole-rock major and trace element compositions of one basalt, one diabase, and 21 rocks from the magmatic-plutonic units of the North Arm Mountain massif, Bay of Islands ophiolite, Newfoundland, were determined. Mineral compositions of a subset of the plutonic rocks were also determined.

The major and trace element compositions of the basalt and diabase are similar to abyssal tholeiites, and this is consistent with the REE data of Malpas (1978) and Suen, et. al. (1979) that suggest the lavas and dikes formed from a depleted or slightly enriched abyssal tholeiitic magma. The alkaline nature of the magma proposed by several previous investigators based on major element chemistry is attributed to alteration.

The major primary minerals of the plutonic rocks are approximately in chemical equilibrium with each other, and mineral zoning, where present, is normal. This indicates that the plutonic rocks formed mainly by in situ nucleation and crystallization on or near the margins of the magma chamber rather than by homogeneous nucleation and gravitational sorting.

Methods of estimating the amount of trapped liquid in plutonic rocks from incompatible trace element concentrations are discussed. Textures and estimates of trapped liquid indicate many of the plutonic rocks from the area of North Arm Mountain from where the rocks in this study were collected are mesocumulates. This and the thinning of the layered units and thickening of the isotropic gabbros suggest the plutonic rocks in this area formed under conditions of faster cooling than did those to the northeast and southwest.

Whole-rock and cryptic mineral variations with pseudo-stratigraphic

height suggest the magma chamber was vertically zoned, with the degree of differentiation increasing upward, but that the extent of fractionation was rather limited. Olivine Fo, plagioclase Ca#, and clinopyroxene Mg# varied by 9, 17, and 13 units, respectively, through a vertical distance of 6 km. through the transition zone and gabbroic units.

Mineral compositions determined in this study and others and the gross lithologic layering suggest the general crystallization order of the North Arm parent magma was olivine ( $\pm$  chromite) - clinopyroxene - plagioclase - orthopyroxene. This is inconsistent with phase relations of abyssal tholeiites in which clinopyroxene crystallizes after olivine and plagioclase. No explanation is suggested.

Most chemical and mineralogic features of North Arm Mountain plutonic rocks can be attributed to a combination of crystal fractionation and repeated mixing of newly injected parent magma in a large, steady-state chamber at an oceanic spreading center. This is consistent with the geologic evidence (Casey, 1980). However, other processes must be responsible for some of the minor variant mineral assemblages in the plutonic rocks.

## ACKNOWLEDGMENTS

I gratefully acknowledge the contributions of the following people: Dr. S.E. DeLong served as advisor and procured funds for the analytical work; Dr. J. Casey provided the samples and many personal observations of the NAM massif; Drs. W.S.F. Kidd and J.F. Bender reviewed the manuscript and made valuable suggestions for its improvement; K. Davis, D. Elthon, and B. Idleman provided technical assistance in the operation of the microprobes; P. Lyman performed the H<sub>2</sub>O analyses; K. McCarthy typed the thesis.

Foremost, I thank my wife, Nancy, whose encouragement, patience, and love contributed immeasurably to the completion of this work.

## TABLE OF CONTENTS

ABSTRACT	ii
ACKNOWLEDGMENTS	v
LIST OF FIGURES	ix
LIST OF TABLES	x
INTRODUCTION	1
TERMINOLOGY	2
CHAPTER I. GEOLOGY	3
1.1 Regional geology	3
1.2 Tectonic interpretation	4
1.3 Local geology of the Bay of Islands ophiolite	4
1.4 Geology of North Arm Mountain	5
CHAPTER II. TEXTURES, CRYSTALLIZATION PROCESSES, AND THEIR BEARING ON CHEMICAL INTERPRETATION	11
2.1 Introduction	11
2.2 Adcumulus textured rocks	11
2.3 Orthocumulus textured rocks	14
CHAPTER III. CHEMISTRY: METHODS AND RESULTS	19
3.1 Sample preparation	19
3.2 Whole-rock chemistry	20
3.2.1 Major elements	20
3.2.2 Trace elements	31
3.2.2.1 Analytical procedure	31
3.2.2.2 Precision, accuracy, and detection limits	31
3.3 Mineral analyses	41

CHAPTER IV.	DISCUSSION OF CHEMICAL OBSERVATIONS	52
4.1	Chemical classification of the Bay of Islands	52
	Magma	
4.2	Estimation of proportion of trapped liquid/primocrysts in North Arm adcumulus textured rocks	58
4.3	Mineral accumulation versus <u>in situ</u> crystallization	64
4.4	Evidence of chemical zonation and magma mixing within a steady-state magma chamber	71
4.4.1	Whole-rock chemical variation in North Arm Mountain plutonic rocks	71
4.4.2	Cryptic chemical variation - Evidence for magma mixing and chemical zonation	77
CHAPTER V.	NORTH ARM MOUNTAIN MINERAL ASSEMBLAGES	81
5.1	Introduction	81
5.2	Crystallization sequence of the North Arm Mountain parent magma	81
5.3	Magma chamber processes inferred from North Arm Mountain mineral assemblages	84
5.3.1	Main sequence assemblages	84
5.3.2	Variant mineral assemblages	86
5.3.2.1	Variability in parent magma composition	87
5.3.2.2	Mixing of evolved liquids	88
5.3.2.3	Disequilibrium crystal fractionation and diffusion and discontinuous	90



nucleation effects on mineral  
assemblages

5.4 Conclusions	91
CHAPTER VI. SUMMARY AND SUGGESTIONS FOR STUDY	93
REFERENCES CITED	96
APPENDIX PETROGRAPHIC DESCRIPTIONS	103

## LIST OF FIGURES

<u>FIGURE NUMBER</u>		<u>PAGE</u>
1	Sample location and simplified geologic map of the North Arm Mountain massif	6
2	Photomicrograph of adcumulus textured olivine gabbro 308A	13
3	Photomicrograph of orthocumulus textured ferrogabbro 123B	15
4	Selected mineral chemical features of North Arm Mountain plutonic rocks	51
5	FeO*/MgO of coexisting olivines and clino- pyroxenes versus FeO*/MgO of liquids presumed in equilibrium with these minerals	67
6	Photomicrograph of "pore" plagioclase in lherzolite 909A	70
7	Variation in whole-rock FeO*/MgO and Zr with height in the NAM plutonic complex	73
8	Correlation between olivine and whole-rock FeO*/MgO of adcumulus-mesocumulus textured rocks of North Arm Mountain	75
9	Cryptic variation in olivine Fo and plagioclase Ca# with height in the NAM plutonic complex	79
10	Diagrammatic representation of the overall crystallization sequence of the North Arm Mountain parent magma	85

## LIST OF TABLES

<u>TABLE NUMBER</u>		<u>PAGE</u>
I	Whole-rock major element compositions of North Arm Mountain rocks	21
II	Electron microprobe operating conditions (whole-rock)	25
III	Whole-rock standards	26
IV	Accuracy of check-standards whole-rock analyses	28
V	Comparison of UMA and LDGO analyses of three North Arm Mountain plutonic rocks	29
VI	Trace element calibration standards and curve statistics	32
VII	Trace element precision estimates	34
VIII A	Recommended trace element standard concentrations	35
VIII B	Accuracy and detection limits of trace element analyses	36
IX	Trace element concentrations of NAM rocks	37
X A	Plagioclase compositions of selected North Arm Mountain plutonic rocks	42
X B	Clinopyroxene compositions of NAM plutonic rocks	43
X C	Hornblende compositions of NAM plutonic rocks	44
XI	Estimated accuracy of LDGO mineral analyses	45
XII	Olivine compositions of selected NAM rocks	46
XIII	Supplemental semi-quantitative mineral chemistry	47

## LIST OF TABLES (continued)

<u>TABLE NUMBER</u>		<u>PAGE</u>
XIV	Selected analyses of ocean-floor and ophiolite rocks	54
XV	Estimated proportions of trapped liquid in some NAM plutonic rocks	61
A I	Modal mineralogy	107
A II	Chart of comparative petrography	108

## INTRODUCTION

The ocean crust and the accretionary process at a divergent plate boundary are of great interest because they provide a window to the character and processes of the upper mantle. However, studies of the ocean crust are limited to direct sampling and viewing of the uppermost portions of the crust and to seismic studies of the deeper section.

It has become fairly well accepted that many ophiolites are remnants of marginal basin or oceanic crust and upper mantle that have been tectonically obducted onto continental margins. This hypothesis is supported by lithologic, structural, geophysical, and chemical data, and if true, these ophiolites provide a unique opportunity to directly study a larger portion of the crustal section and upper mantle than is possible by undersea study.

The Bay of Islands ophiolite in Newfoundland is very well preserved and exposed, and data so far are consistent with an ocean floor origin. This study examined some of the chemical features of pluto-magmatic rocks from the North Arm Mountain (NAM) massif of this ophiolite for the purpose of 1) classifying the parent magma to determine if an ocean floor origin is supported, 2) determining the character of chemical variations in the plutonic rocks to elucidate possible magma chamber and crystallization processes, and 3) determining if these chemical variations fit or suggest new constraints for models of divergent plate accretion.

## TERMINOLOGY

To avoid confusion, an explanation of the use of certain terms is necessary. Parent magma is used to describe the magma entering the subcrustal chamber. This is opposed to the usage describing the liquid derived from melting in the mantle. This latter liquid may or may not undergo compositional modification during ascent, and hence the need to define the term.

Local liquid is used to describe the liquid which in any way is directly involved in the crystallization of a single small scale rock. The need for this term is because the composition of the magma as a whole may not be homogeneous, and discussions involving rock forming processes need to specify conditions of the liquid directly responsible for the composition of the rock.

The terms primocryst or primary crystal mean the liquidus phase or phases in the strict sense, or loosely any major mineral which co-crystallized with the liquidus phases by the same process, i.e., by the same degree of diffusional contact with the local magma. These terms are used in place of the term cumulus crystal to avoid the implication that gravitational accumulation took place. Primocrysts are distinct from crystals formed from liquid wholly or partly trapped interstitial to the primocrysts. These are referred to as interprecipitate crystals in place of the term intercumulus.

## CHAPTER 1

### GEOLOGY

#### 1.1 REGIONAL GEOLOGY

A detailed review of western Newfoundland geology, including descriptions of litho-stratigraphic units and tectonic interpretations, can be found in Williams (1975). The following summary is based on that paper and also Stevens (1970), Church and Stevens (1971), Dewey and Bird (1971), Kennedy (1973), Williams (1973), and Williams and Stevens (1974).

The Bay of Islands (BOI) ophiolite complex lies within the uppermost slice of a series of five recognized allochthonous slices known collectively as the Humber Arm Allochthon. This allochthon is located in the southwestern part of the Newfoundland geologic province known as the Western Platform, which is separated from the rest of Newfoundland by the Cabot Fault. A correlative allochthon in the northern part of the province is the Hare Bay Allochthon, which also contains a probable ophiolite remnant (White Hills Peridotite) in the uppermost slice. The lower slices in both allochthons are composed mostly of clastic sedimentary rocks and have been interpreted as having originated in a continental rise setting. The basement of the Western Platform is precambrian gneiss. An autochthonous sequence of clastic and carbonaceous sedimentary rocks lies unconformably on the basement and separates it from the allochthon. The Long Point Formation (late to middle Ordovician age) unconformably overlies both the allochthonous and autochthonous rocks.

## 1.2 TECTONIC INTERPRETATION

Most recent interpretations of the tectonic evolution of the Western Platform suggest that most of the autochthonous and allochthonous rocks originally formed on the stable, east-facing North American continental margin during Cambrian-early Ordovician time. Some geologists (e.g., Church and Stevens, 1971; Nelson and Casey, 1979), based on the age difference between ophiolite rocks and rift dike rocks in the continental margin, believe the ophiolite formed at a considerable distance from the continental margin. Closing of an ocean to the east of the margin resulted in emplacement of the allochthons, including the ophiolites. Final emplacement must have occurred no later than late-Ordovician time (Llandelian-Caradocian) because this is the age of fossils in the overlying neo-autochthonous Long Point Formation. The major interpretive differences include subduction direction and source region of the allochthonous rocks (Dewey and Bird, 1971; Church and Stevens, 1971; Strong, 1974; Williams, 1975; Malpas, 1979; Nelson and Casey, 1979).

The ages of all the structural slices are not known. However, from those that are known, most geologists suggest that the highest slices originated farthest east, so that a section upward through the allochthon broadly represents a west-to-east traverse of the original continental margin and adjacent oceanic crust.

## 1.3 LOCAL GEOLOGY OF THE BAY OF ISLANDS OPHIOLITE

The Bay of Islands ophiolite complex, approximately 100km x 25km, consists of the Table Mountain (TM), North Arm Mountain (NAM), Blow-Me-



Down Mountain (BMDM), and Lewis Hills (LH) massifs. The Blow-Me-Down and North Arm massifs are the most complete, exhibiting all typical ophiolite lithologies. Overlying sedimentary rocks are probably para-llochthonous (Kidd and Casey, 1981). The Lewis Hills massif contains a zone of highly deformed mafic and ultramafic rock which is continuous with the Coastal Complex and which has been interpreted as a fossil transform zone (Karson, 1977; Karson and Dewey, 1977). Within and between these massifs, the lithologies, structure, and unit thicknesses vary considerably (Casey et al., 1980). These authors do not believe this variability is inconsistent with available ocean crust data, and in fact propose that such variability is a fundamental aspect of the oceanic crust.

#### 1.4 GEOLOGY OF NORTH ARM MOUNTAIN

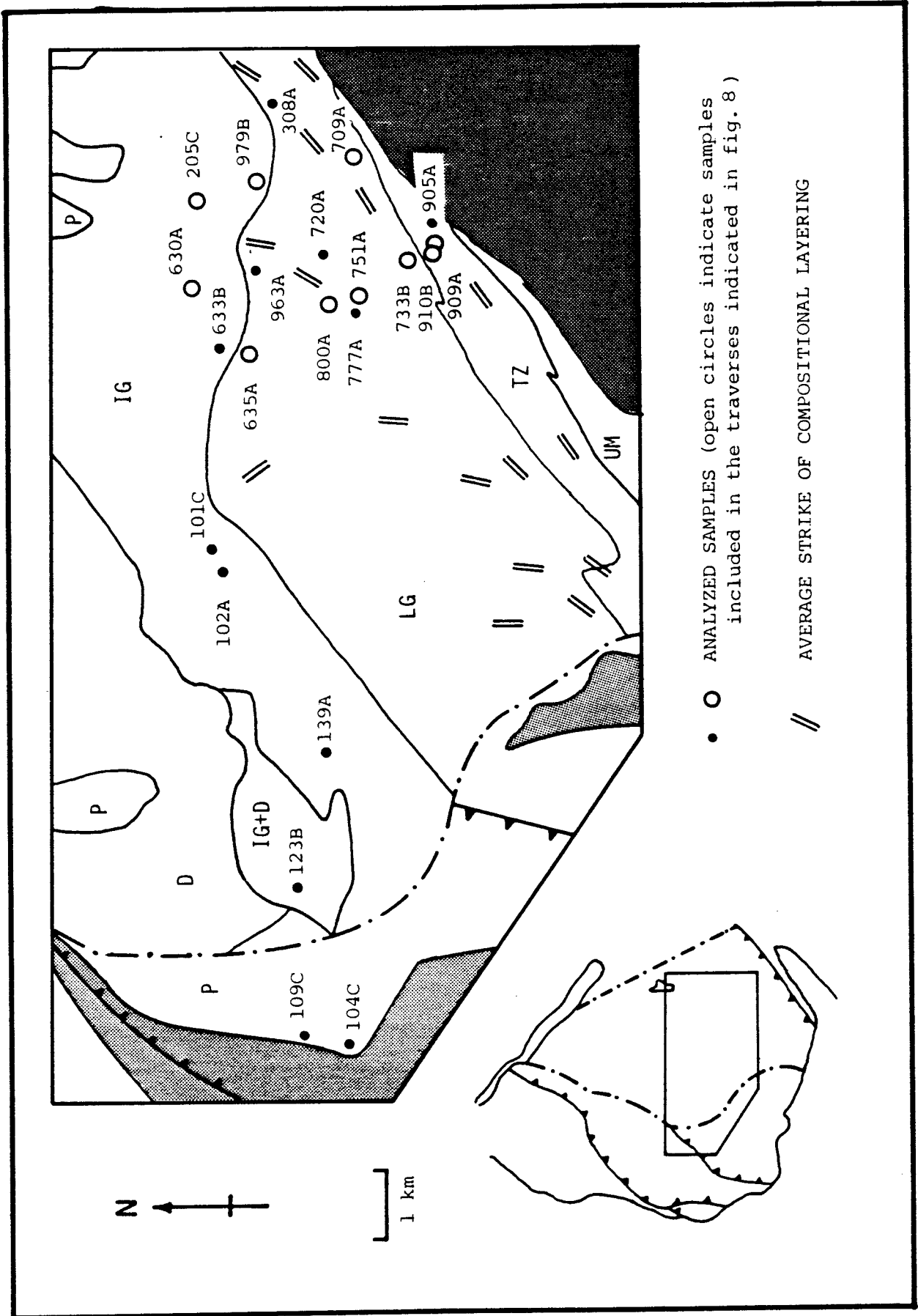
This study is primarily concerned with the North Arm massif and follows Casey's (1980) mapping and descriptions of the lithologic units. Samples were provided by J. Casey (see fig. 1 for locations). The following description of the major litho-structural units, from bottom to top, is condensed from Casey, with greatest emphasis on the magmatic-plutonic sequence.

##### UPPER MANTLE

###### Harzburgite tectonite

This unit, first proposed to be a residuum of partial melting of upper mantle by Irvine and Findlay (1972), is mostly harzburgite with minor dunite and orthopyroxenite. It has a tectonized fabric which is

Figure 1. Simplified geologic map of a portion of the North Arm Mountain massif (modified from Casey, 1980) with locations of samples discussed in this study. Samples included in the two traverses indicated in figure 8 are represented by open circles, all others by solid dots. The short double lines indicate the average strike (visually estimated from Casey's map) of compositional layering. Fine stiple = parallochthonous sedimentary rocks; dark stiple = harzburgite; unadorned = magmatic complex. P = pillow lavas; D = diabase dikes; IG = isotropic gabbroic rocks; LG = layered gabbroic rocks; TZ = transition zone rocks; UM = magmatic ultramafic rocks.



generally thought to have resulted from solid state deformation. Deformational and cross-cutting relationships suggest that the dunite and pyroxenite had a magmatic origin coeval with the deformation of the harzburgite. Lherzolite is found locally near the basal metamorphic aureole and may represent undepleted or less depleted mantle material.

#### MAGMATIC-PLUTONIC COMPLEX

##### Ultramafic and Transition Zones

The magmatic plutonic rocks of NAM are composed mainly of combinations of olivine, plagioclase, and clinopyroxene, with lesser amounts of spinel, orthopyroxene, and brown hornblende. The basal rocks are usually ultramafic, commonly with dunite at the bottom which becomes increasingly interlayered upward with clinopyroxene bearing rocks (clinopyroxenites and wehrlites) and with minor amounts of orthopyroxene bearing rocks (websterites, harzburgite lenses).

The ultramafic rocks grade upward into mafic gabbroic rocks by increased interlayering of feldspathic lithologies. This gradational zone has been named the transition zone by Casey (1980) and is called the critical zone by most Newfoundland geologists. This and the ultramafic zone pinch out in the northeastern part of Casey's map area where gabbro conformably contacts residual harzburgite for about 4km along strike of the contact. The units reappear further northeast (Rosencrantz, 1979).

## Gabbros

Gabbros on NAM are mapped as two distinct types based on presence or absence of igneous layering. The lower gabbro is layered and is mainly olivine gabbro and gabbro, with minor troctolite, anorthosite, and feldspathic wehrlite. The layered gabbro unit thins considerably in the area where it is in contact with residual harzburgite.

The upper gabbro generally lacks layering and is therefore termed massive or isotropic following the terminology of Dewey and Kidd (1977). Gabbro and olivine gabbro dominate the lower part of this unit, but olivine is sparse in the upper part. Brown hornblende and iron-titanium oxides are more prominent in the upper isotropic gabbro, and occasional orthopyroxene bearing gabbro has been reported in these rocks (Irvine and Findlay, 1972; Church and Riccio, 1977). The contact between layered and isotropic gabbro is diffuse, with layering gradually dying out upward. The isotropic gabbro unit thickens where the ultramafic and transition zone units pinch out.

## Igneous Layering

The layering in the NAM magmatic-plutonic rocks is most commonly the uniform type with sharp contacts defined by abrupt changes in mineral proportions or assemblages. Layering defined by abrupt changes in grain size and texture is also present. Mineral grading is minor and size grading is nearly absent. The layering is laterally discontinuous, often on outcrop scale, but the overall sense of orientation is arcuate, with layering roughly parallel to the major lithologic boundaries near the base of the magmatic complex, and curving to roughly perpendicular to major lithologic boundaries at the

top of the layered gabbro.

#### Extrusive and Hypabyssal Units

These units consist of massive diabases and diabase dikes overlain by metabasaltic pillow lavas and breccias. They have greenschist or lower amphibolite facies mineral assemblages, a feature common in ophiolitic and ocean floor basalts and diabases.

The average strike of the nearly vertical sheeted dikes is NW-SE, suggestive of a NE-SW spreading direction. Rosencrantz (1979) has determined from chilled margin statistics that the presumed ridge axis was southwest of the ophiolite complex.

## CHAPTER II

### TEXTURES, CRYSTALLIZATION PROCESSES, AND THEIR BEARING ON CHEMICAL INTERPRETATION

#### 2.1 INTRODUCTION

Recognition of two basic plutonic rock textural types, orthocumulates and adcumulates, and their variants in the pluto-magmatic sections of various ophiolites has placed important constraints on possible crystallization processes operating in oceanic spreading center magma chambers. A general consideration of these textures and processes is necessary as a basis for evaluating chemical features of these rocks. Discussion of how NAM data relate to these processes will be presented in later sections.

The "cumulate" textural terminology of Wager, et al. (1960) is retained for descriptive purposes. Implicit in the terms orthocumulus and adcumulus is the relative degree of equilibrium between the local magma and the interprecipitate liquid of the forming rocks. However, use of this terminology in this discussion does not imply accumulation of primary crystals by physical transport. The question of whether the primary crystals of these rocks crystallized in situ or accumulated by physical transport is a factor bearing on the interpretation of chemical data. This question is discussed in section 4.3.

#### 2.2 ADCUMULUS TEXTURED ROCKS

Adcumulate is the predominant textural type in all but the upper isotropic gabbros of several ophiolites. These rocks are composed of

varying proportions of unzoned anhedral olivine, pyroxene, plagioclase, and spinel primocrysts with mutually interfering margins and only minor, if any, material interstitial to the primocrysts (see figure 2). This texture is believed to form when the chemical diffusion rate is fast enough relative to crystallization rate (Campbell, 1978) or settling rate (e.g., Wager et al., 1960) so that equilibrium is maintained between the liquidus primocrysts and the local magma. Thus incompatible elements continually diffuse out of or away from the incipient rock as the primocrysts enlarge by addition of material with the same composition as the primocrysts. The very low concentration of incompatible elements is often cited as evidence of this process (e.g., Stern, 1979; McBirney and Noyes, 1979).

Interpretation of chemical features of adcumulates is fairly straightforward. It is quite obvious that compositions of rocks formed by adcumulus processes are not equal to liquid compositions but are weighted sums of liquidus mineral compositions plus very minor components of trapped liquid. Factors affecting whole rock concentrations of all elements include their concentrations in the local liquid and partition coefficients. Concentrations of elements incompatible with primocryst phases will also heavily depend on the amount of trapped pore liquid, while trace elements compatible with primocryst phases will depend heavily on the presence and proportion of host primocrysts. Whole rock compositions of adcumulates are therefore not too useful for determining liquid compositions (however, see sections 4.3 and 4.4.1).

Because adcumulus crystallization is believed to be approximately an equilibrium process, inferences about the liquid composition can be made from known partition coefficients. Unfortunately, partition coefficients of many primocryst forming components vary with such



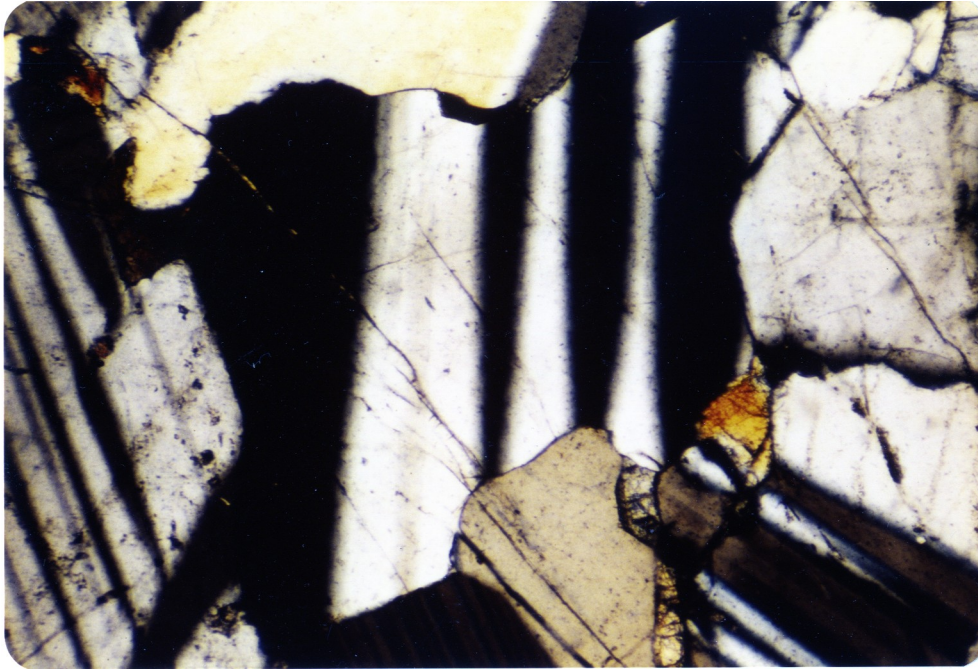


Figure 2. Sample 308A, crossed nicols. Photomicrograph showing the general adcumulus nature of plagioclase crystals with interlocking boundaries. The small intercumulus grains of olivine are typical of many adcumulus-mesocumulus textured samples in this study. Olivine is a major primary phase elsewhere in this slide, suggestive of co-precipitation of olivine and plagioclase.

parameters as temperature, pressure, and composition. Therefore, variations in these parameters within the magma chamber limit our ability to infer chemical features of the magma. One feature of the local liquid which can be inferred with reasonable confidence from olivine compositions is  $\text{FeO}^*/\text{MgO}$ , because  $K_D^{\text{ol/liq}}$  is fairly constant over a range of pressure and temperature (Roeder and Emslie, 1970). Also, anorthite content of plagioclase should indicate relative degrees of fractionation of liquids in equilibrium with the plagioclases, although not as reliably as olivine because the distribution coefficients of the components of plagioclase are more variable (Drake, 1976). This is also true of pyroxenes.

### 2.3 ORTHOCUMULUS TEXTURED ROCKS

Orthocumulus textured rocks occur on NAM (Casey, 1980) and other ophiolites, for example the Oman (Pallister and Hopson, 1981; Smewing, 1981) and Chilean ophiolites (Elthon, personal communication, 1981; Stern, 1979), in the upper isotropic gabbros near the diabase-isotropic gabbro interface. Texturally these rocks are composed of a network of euhedral to subhedral primary crystals with considerable material interstitial to these primary crystals (figure 3). The primary crystals are usually normally zoned and the interstitial material is generally lower in the reaction series.

Crystal zoning and the apparent abundance of trapped liquid suggest that equilibrium between the primocrysts and the local magma was not maintained as in adcumulates. This is believed to indicate a faster crystallization rate relative to diffusion rate compared to adcumulates. Based on this and the location of orthocumulates in ophiolites, several geologists (e.g., Stern, 1981; Casey, 1980;

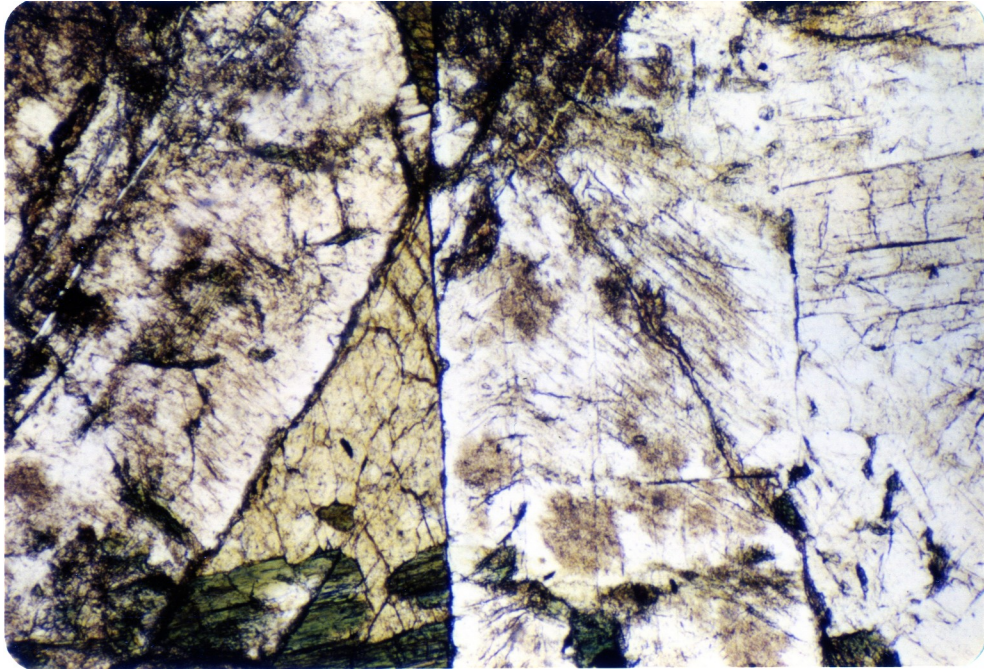


Figure 3. Sample 123B, plane light. Photomicrograph showing orthocumulus texture with amphibole (note cleavage) interstitial to interlocking subhedral-euhedral plagioclase laths. Note that the more sodic rims of the zoned plagioclase are less altered than the more calcic cores.

Pallister and Hopson, 1981) support the hypothesis that orthocumulates formed by underplating on the roof of a large magma chamber under conditions of rapid heat loss. Although they didn't distinguish between orthocumulates and adcumulates, Dewey and Kidd (1977) suggested the isotropic gabbros as a whole formed by plating on the roof or walls of the chamber.

Interpretation of chemical features of orthocumulates is somewhat more difficult than adcumulates. The same factors controlling compositions of adcumulates (e.g.,  $K_D$  variability, liquid composition, percent trapped liquid) apply to orthocumulates, with the additional complication of uncertainty in the degree of equilibrium maintained with the local magma. Variations in the relative crystallization and diffusion rates may be expected to yield rocks which maintained different degrees of equilibrium with the magma. The greater the crystallization rate relative to diffusion rate, the closer a closed system is approached in which most of the primocryst components come from the interstitial liquid, while the greater percentage of incompatible elements are trapped before they can diffuse out of the rock. The limiting case would be quickly cooled fine grained rocks such as the diabases or basalts. At the other end of the spectrum an adcumulus or open system may be approached (Casey, 1980). Furthermore, diffusion rates vary among elements and therefore the degree of equilibrium among elements may vary within individual samples.

Elthon (personal communication, 1981) has observed a distinct difference in the Zr content between upper orthocumulus textured gabbros and deeper adcumulate gabbros. He has interpreted this to be due to a

greater amount of trapped liquid in the orthocumulates than the adcumulates. Also, the orthocumulate ferrogabbro 123B in this study has significantly higher concentrations of incompatible elements than the adcumulate samples. Elthon estimates that the amount of trapped liquid in the orthocumulate gabbros is in the range 20-40%, and 5-10% for the adcumulates. However, these estimates do not take into account the Zr component contained in minerals. Clinopyroxene and hornblende can contribute significantly to the whole-rock Zr content ( $K_{\text{Cpx}/1} = 0.1$ ,  $K_{\text{hb}/1} = 0.5$ ; Pearce and Norry, 1979). Nevertheless, there appears to be a significant difference in the amount of trapped liquid between the two rock types in Tortuga. Additional modelling of this type based on other incompatible elements and empirically determined partition coefficients of mineral separates may provide fairly accurate estimates of the amount of trapped liquid.

In view of these considerations, it appears that whole-rock chemistry does not directly represent liquid compositions. Nevertheless, some useful information may be inferred from this information.

If the primary crystals of orthocumulates do not significantly re-equilibrate with the changing composition of the surrounding liquid, then the compositions of the cores of these minerals can be used to infer chemical features of the local magma as in the adcumulates. Significant re-equilibration seems unlikely because of the marked zoning, and the fact that this would require some degree of solid state diffusion which is certainly slower than diffusion in the liquid. It has already been established that crystallization takes place fast enough to prevent equilibrium diffusional contact with the local magma, so it seems likely that crystallization of trapped pore

liquid would occur before significant re-equilibration with earlier crystals occurs.

One unfortunate feature of orthocumulates in ophiolites is that they often lack olivine, the most reliable indicator of liquid  $\text{FeO}^*/\text{MgO}$ . Determination of this parameter is therefore left to pyroxene which is fairly ubiquitous in these rocks.

## CHAPTER 3

### CHEMISTRY: METHODS AND RESULTS

#### 3.1 SAMPLE PREPARATION

Samples were chosen for chemical analysis on the basis of freshness in thin section. Most specimens were large enough (6 or 7 cm in the smallest dimension) to homogenize small scale layering effects.

Samples were coarsely broken with a hydraulic splitter, and pieces with weathering rind, saw marks, and macroscopic veins were discarded. The freshest pieces were further crushed in a "chipmunk" hopper, followed by pulverization between tungsten steel rollers. Final powdering to pass a 400 mesh screen was done in a tungsten carbide mixing mill for 20 minutes.

Glass beads for major element electron microprobe analyses were prepared by direct fusion of rock powder in a molybdenum strip furnace in an argon atmosphere. The molybdenum strips were first cleaned with xylene and acetone, and degassed in the argon atmosphere at an estimated 800-900° C. Rock powders were fused at an estimated 1400-1500° C for 6-8 seconds, then quenched by rapid reduction in argon pressure. To insure homogeneity, the glass beads were ground in an agate mortar and re-fused before being mounted in epoxy and polished to approximately 1 micron. Two ultramafic samples, wehrlite 905A and lherzolite 909A, formed "skins" of quench crystals following this procedure. To alleviate this problem, these samples were mixed with equal weights of dried  $\text{LiBO}_4$  flux and fused at a lower temperature (estimated at about 900° C) than the other samples.

Trace element analyses were done by x-ray fluorescence on pressed powder pellets. Splits of the 400 mesh powders were pressed in boric acid jackets at about 12 tons per square inch.

Whole rock  $H_2O^+$  analyses were performed by Peter Lyman following the procedure of DeLong and Lyman (in press). Polished thin sections for mineral analyses were prepared by Western Petrographic Company.

### 3.2 WHOLE ROCK CHEMISTRY

#### 3.2.1 Major elements

Seventeen samples were analyzed with the ARL electron microprobe at Lamont Doherty Geological Observatory, and eight samples were analyzed with the ETEC instrument at the University of Massachusetts, Amherst. Three samples were analyzed with both probes for comparison. Results, operating conditions, and calibration standards are listed in tables I-III. Samples designated with a U in table 1 were analyzed with the UMA instrument.

Most of the analyses done at LDGO are averages of 10 analyzed points. Most of these samples included a traverse of several points across the glass bead, and no systematic variations were observed along these traverses. Because no consistent or significant differences in either the mean or standard deviation were observed between the first 5 spots and the full 10 spots, it was concluded that 5 points were sufficient to determine the average composition of these beads. The analyses reported for samples analyzed with the UMA probe are averages of 5 spots.



TABLE I

## WHOLE-ROCK MAJOR ELEMENT COMPOSITION (WT. % OXIDE)

SAMPLE	101C	102A	104C	109C	123B	139A	205C
ROCK TYPE	TR	OG	BA	DI	FG	G	OG
PROBE	U		U		U		
SiO <sub>2</sub>	77.31	49.15	50.59	49.66	46.10	50.75	49.84
TiO <sub>2</sub>	0.12	0.21	1.93	1.44	2.96	0.36	0.43
Al <sub>2</sub> O <sub>3</sub>	12.06	24.18	15.31	17.58	11.37	18.05	16.71
FeO*	0.81	3.93	10.82	9.76	14.97	6.57	6.79
MnO	0.00	0.08	0.24	0.26	0.28	0.13	0.14
MgO	0.12	5.58	7.26	8.47	7.14	9.24	10.00
CaO	0.77	14.41	5.60	8.82	11.30	11.97	13.48
Na <sub>2</sub> O	4.52	2.36	4.37	3.06	1.60	2.81	2.46
K <sub>2</sub> O	0.07	0.03	0.34	0.54	0.07	0.19	0.02
P <sub>2</sub> O <sub>5</sub>	n.d.	0.12	n.d.	0.20	n.d.	0.09	0.13
TOTAL	95.78	100.07	96.46	99.79	95.79	100.16	100.00
H <sub>2</sub> O <sup>+</sup>	0.40	2.28	3.70	3.30	1.43	2.31	1.45
H <sub>2</sub> O <sup>-</sup>	0.24	n.d.	1.10	0.64	0.14	0.43	0.30
FeO*/MgO	6.75	0.70	1.49	1.15	2.10	0.71	0.68

TABLE I (continued)

SAMPLE	308A	630A	633B	635A	709A	720A	733B
ROCK TYPE	OG	OG	MG	TROC	OG	OG	OG
PROBE					U		
SiO <sub>2</sub>	47.48	49.91	49.05	48.42	48.87	47.17	48.73
TiO <sub>2</sub>	0.12	0.30	0.72	0.15	0.18	0.38	0.17
Al <sub>2</sub> O <sub>3</sub>	19.03	20.18	19.44	19.97	20.40	26.82	21.27
FeO*	4.69	6.06	8.90	6.00	4.17	3.53	3.88
MnO	0.08	0.11	0.14	0.11	0.04	0.10	0.08
MgO	14.05	8.24	8.29	11.97	8.76	5.07	7.91
CaO	13.82	13.13	11.07	11.25	15.07	14.59	15.47
Na <sub>2</sub> O	0.93	2.41	3.13	2.13	1.31	2.17	1.89
K <sub>2</sub> O	0.00	0.01	0.05	0.07	0.01	0.02	0.00
P <sub>2</sub> O <sub>5</sub>	0.09	0.09	0.12	0.10	n.d.	0.10	0.10
TOTAL	100.29	100.44	100.91	100.17	98.81	99.95	99.50
H <sub>2</sub> O <sup>+</sup>	2.66	0.89	3.05	3.24	1.14	1.37	1.07
H <sub>2</sub> O <sup>-</sup>	0.50	0.36	0.30	0.72	0.26	0.22	0.15
FeO*/MgO	0.33	0.74	1.07	0.50	0.48	0.70	0.49

TABLE I (continued)

SAMPLE	751A	764C	777A	800A	905A	
OCK TYPE	OG	OG	Hb-OG	OG	WEHRLITE	
PROBE	U				U	
SiO <sub>2</sub>	47.28	51.84	46.66	47.68	51.71	50.62
TiO <sub>2</sub>	0.26	0.16	1.38	0.29	0.13	0.08
Al <sub>2</sub> O <sub>3</sub>	19.75	21.05	16.83	20.45	2.68	2.23
FeO*	5.78	2.95	9.42	5.31	5.51	5.27
MnO	0.18	0.10	0.20	0.11	0.13	0.07
MgO	11.58	6.62	8.57	9.77	21.77	20.60
CaO	12.57	14.86	12.99	14.08	17.81	17.83
Na <sub>2</sub> O	1.34	2.02	2.88	1.76	0.22	0.00
K <sub>2</sub> O	0.01	0.00	0.07	0.00	0.00	0.00
P <sub>2</sub> O <sub>5</sub>	n.d.	n.d.	n.d.	n.d.	n.d.	n.d.
TOTAL	98.75	99.60	99.00	99.45	99.86	96.70
H <sub>2</sub> O <sup>+</sup>	1.57	n.d.	0.97	1.14	2.81	
H <sub>2</sub> O <sup>-</sup>	0.17	n.d.	0.16	0.14	0.64	
FeO*/MgO	0.50	0.45	1.10	0.54	0.25	0.26

TABLE I (continued)

SAMPLE	909A	910B	963A		979B	
ROCK TYPE	LHERZ	OG	OG		OG	
PROBE	U		U		U	
SiO <sub>2</sub>	48.48	50.39	49.27	50.18	45.25	47.63
TiO <sub>2</sub>	0.34	0.20	0.75	0.72	0.20	0.10
Al <sub>2</sub> O <sub>3</sub>	3.00	19.25	15.82	15.04	27.21	24.73
FeO*	8.82	3.83	6.71	6.38	4.23	4.10
MnO	0.21	0.12	0.14	0.17	0.07	0.10
MgO	21.89	9.31	9.04	8.55	6.87	6.70
CaO	14.20	14.63	14.51	14.87	13.23	13.67
Na <sub>2</sub> O	0.00	1.81	2.61	1.71	1.90	1.46
K <sub>2</sub> O	0.00	0.01	0.01	0.01	0.01	0.01
P <sub>2</sub> O <sub>5</sub>	n.d.	n.d.	n.d.	n.d.	n.d.	n.d.
TOTAL	96.94	99.55	98.91	97.63	98.97	98.50
H <sub>2</sub> O <sup>+</sup>	1.08	0.84 <sup>1</sup>	0.86		1.27	
H <sub>2</sub> O <sup>-</sup>	0.20		0.11		0.23	
FeO*/MgO	0.26	0.41	0.74	0.75	0.62	0.61

Notes: Analyses performed with the UMA microprobe are designated U, all others were done with the LDGO probe. Samples 905A, 963A, and 979B were analyzed with both probes. Not determined- n.d.. Rock type abbreviations: TR- trondhjemite, TROC- troctolite, BA- basalt, DI- diabase, G- gabbro, OG- olivine gabbro, MG- metagabbro, FG- ferrogabbro, LHERZ- lherzolite.

1. Total water.

TABLE II

## ELECTRON MICROPROBE OPERATING CONDITIONS (WHOLE-ROCK)

INSTRUMENT	LDGO	UMA
TYPE	ARL	ETEC
ACCELERATING VOLTAGE	10 kv	15 kv
BEAM DIAMETER (approx.)	15-20 $\mu\text{m}$	15-20 $\mu\text{m}$
CORRECTION PROCEDURE	Bence-Albee	Bence-Albee

TABLE III

## WHOLE-ROCK STANDARDS

OXIDE	LDGO STANDARDS		UMA STANDARDS	
TiO <sub>2</sub>	Ilmenite	28.58	Mn-ilmenite	45.70
MnO	Rhodenite	28.53	Mn-ilmenite	5.00
FeO*	Hematite	69.86	Mn-ilmenite	46.83
SiO <sub>2</sub>	Wakefield Diopside	55.37	Jadeite-35	56.88
Na <sub>2</sub> O	Sanidine	2.23	Jadeite-35	5.36
K <sub>2</sub> O	Sanidine	10.04	Sanidine	13.10
MgO	Periclase	60.32	Cr-Cats	17.88
CaO	Hakone Anorthite	13.49	Cr-Cats	25.79
Al <sub>2</sub> O <sub>3</sub>	Hakone Anorthite	18.92	Anorthite	36.64
P <sub>2</sub> O <sub>5</sub>	Apatite	17.86	-----	

Whole-rock analyses done with the UMA probe are probably more accurate and internally consistent than those done with the LDGO probe. All analyses done at UMA were done at one time. The instrument was very stable and re-standardization was not necessary. Two points each on standards Mn-Ilm and JD-35 were analyzed after half the NAM samples were analyzed, and the means and percent deviations from recommended values are listed in table IV. These provide an indication of accuracy at the concentration levels of these standards.

The LDGO analyses were done at several different times, and the stability of the instrument was variable. Because of this, a general estimate of accuracy and precision is difficult to make and varied among samples run at different times. The Kakanui Kaersutite standard was used as the main check standard, and additional checks were occasionally done on other standards. The means of 4 checks on the kaersutite (each check representing the average of 2-3 points) are listed in table IV, as are the standard deviations and percent deviations from the recommended values. Significantly larger deviations were noted on checks of standards at low concentrations. For example, note that although the percent deviation of the mean of MnO is only 5.5% greater than the recommended value for the kaersutite, the standard deviation is 50% of the mean. The accuracy of MnO and  $P_2O_5$  is estimated at about  $\pm 50\%$ .

Table IV shows that the accuracy of analyses done with the LDGO probe is not as good as those done with the UMA probe. Table V shows the percent deviation of three NAM samples run on the UMA probe from their concentrations determined with the LDGO probe. The UMA probe gave consistently lower values for  $TiO_2$ ,  $FeO^*$ ,  $Na_2O$ ,  $MgO$ , and  $Al_2O_3$ , and consistently higher values of  $CaO$ . The results for  $SiO_2$  and

TABLE IV

## ACCURACY OF CHECK STANDARDS WHOLE-ROCK ANALYSES

OXIDE	UMA PROBE			LDGO PROBE <sup>1</sup>		
	STD.	MEAN	% DEV. MEAN	MEAN	STD. DEV.	% DEV. MEAN
TiO <sub>2</sub>	Mn-Ilm	45.25	-1.0	4.82	0.34	-3.6
MnO	Mn-Ilm	4.82	-3.6	0.10	0.05	+5.5
FeO*	Mn-Ilm	46.87	+0.1	10.93	0.33	-1.2
SiO <sub>2</sub>	JD-35	57.37	+0.9	39.95	1.50	-0.6
CaO	JD-35	16.47	-2.1	9.61	0.21	-5.8
Na <sub>2</sub> O	JD-35	5.36	0.0	2.70	0.34	+6.1
MgO	JD-35	12.09	-0.1	12.80	0.20	-0.5
Al <sub>2</sub> O <sub>3</sub>	JD-35	8.87	+0.6	14.76	0.86	+5.8
K <sub>2</sub> O				1.99	0.17	-6.3
P <sub>2</sub> O <sub>5</sub>						

1. All values for the LDGO probe are for the standard Kakanui Kaersutite.

Notes: Standards Mn-Ilm and JD-35 are potassium-free.

P<sub>2</sub>O<sub>5</sub> not determined with the UMA probe.

Kakanui Kaersutite is phosphorus-free.

% Dev. Mean = ((mean-std. conc./std. conc.) x 100).



TABLE V

COMPARISON OF UMA AND LDGO ANALYSES  
OF THREE NORTH ARM MOUNTAIN SAMPLES

OXIDE	963A	905A	979B
TiO <sub>2</sub>	-4.0	-38.5	-50.0
MnO	17.7	-46.2	30.0
FeO*	-4.9	-4.4	-3.1
SiO <sub>2</sub>	1.8	-2.1	5.0
CaO	2.4	0.1	3.2
Na <sub>2</sub> O	-34.5		-23.2
MgO	-5.4	-5.4	-2.5
Al <sub>2</sub> O <sub>3</sub>	-4.9	-16.8	-9.1
K <sub>2</sub> O		0.0	0.0
P <sub>2</sub> O <sub>5</sub>			

Notes: Values are defined as percent deviation of UMA values from

LDGO values.  $((\text{UMA conc.} - \text{LDGO conc.})/\text{LDGO conc.}) \times 100$ .

Phosphorus not determined with UMA probe.

No potassium was detected in sample 963A with either probe.

No sodium was detected in sample 905A.

MnO were variable. The magnitude of the variation among the samples was not consistent, due to the poor reproducibility of the LDGO probe and to the differences in elemental concentrations among the samples (i.e., accuracy is better at higher concentrations).

The UMA analyses consistently totalled lower than the LDGO analyses, and some totals were below the level considered good analyses. However, check analyses of standards provided no ready explanation for this. Although CaO, TiO<sub>2</sub>, and MnO consistently checked low with the UMA probe, only about 1 wt.% total deviation of these three element should be expected at the high concentrations of these check standards. At the generally lower concentrations of the NAM samples, even less deviation is expected, unless the accuracy is significantly worse at lower concentrations.

Part of this problem may be attributed to elements that were not determined by microprobe. For example, sample 909A (total = 96.94) has a high nickel and chromium content (NiO + Cr<sub>2</sub>O<sub>3</sub> = 1 wt.%), and the trondhjemite 101C may be expected to have significant P<sub>2</sub>O<sub>5</sub>, judging by its content of incompatible elements. Nevertheless, these factors do not account for the low totals in all samples.

### 3.2.2 Trace Element Analyses

#### 3.2.2.1 Analytical Procedure

Trace elements were analyzed with the Woods Hole Oceanographic Institution's Phillips AXS automated x-ray fluorescence spectrometer. Operating conditions and techniques are given in Schroeder, et al., (1980) except that the elements Zr, Y, Sr, and Rb were analyzed using a Mo target tube instead of a W tube.

The analyses were carried out in two groups. Calibration standards for one group (Zr, Y, Sr, Rb) were run at the beginning and end of the suite of unknowns, and the means of the two runs were used for calibration. Calibration standards for the other group (Zn, Cu, Ni, Cr, V, Co, Ba, Nb) were run only prior to the unknowns. Standard BR (a basalt) was run after every seven unknowns to check precision. For elements where BR was used as a calibration standard, the means of 29 runs were used. Intensities were corrected for background, peak overlap, and major element mass absorption effects. Calibration standards, peak overlaps, and calibration curve parameters are listed in table VI.

#### 3.2.2.2 Precision, Accuracy, and Detection Limits

Precision was generally very good, although not quite as good as reported in Schroeder, et al., (1980). In the group of samples in which the NAM samples were run, basalt standard BR was run ten times with the first group of elements (Zr, Y, Sr, RB) and fourteen times with the other group of elements. Means, standard deviations, and precision or coefficient of variation (defined as 100 std. dev./mean) of BR runs

TABLE VI

## TRACE ELEMENT CALIBRATION STANDARDS AND CURVE STATISTICS

ELEMENT	Zr	Y	Sr	Rb	Zn	Cu	Ni	Cr	V	Co	Ba	Nb
Calib.	BCR	BCR	BCR	BCR	BCR	BCR	GSP	BCR	BCR	BCR	BCR	BCR
Standards	W-1	GSP	GSP	W-1	GSP	GSP	W-1	W-1	GSP	W-1	W-1	GSP
	35-2	W-1	W-1	AGV	W-1	W-1	AGV	AGV	W-1	AGV	BR	W-1
		AGV	AGV	MRG	DTS	BR	BR	8-2	AGV	PCC	MRG	AGV
					MRG	MRG	MRG	MRG	BR		5D3	
Slope <sub>3</sub> (x 10 <sup>3</sup> )	25.716	9.455	9.342	9.547	2.421	2.533	1.694	2.534	3.584	7.376	222.25	43.879
Intercept (ppm)	17.06	4.31	4.19	0.92	9.49	-67.57	8.31	-17.51	5.54	4.02	-64.83	-2.74
Intercept std. dev.	1.12	3.87	1.62	0.65	1.94	12.37	2.43	1.48	4.16	1.96	3.68	0.79
Corr. Coeff.	1.0000	0.9762	1.0000	0.9998	0.9995	0.9897	0.9996	0.9999	0.9996	0.9990	0.9999	0.9986
Overlap correct.	SrK <sub>a</sub>	RbK <sub>a</sub>						Ti, VK <sub>a</sub>	TiK <sub>a</sub>	FeK <sub>a</sub>		

are listed in table VII. Sample standard deviations were within 2% of the mean except for Co (2.9%) and Zr (5.4%).

For some unknown reason, the first three runs of BR produced significantly higher Zr intensities than the last seven runs. The precision for the last seven runs, during which the NAM samples were run, was much better (std. dev. =  $\pm 2.5$  ppm, or 0.9%). Zirconium also showed the poorest precision (3.8%) in the BR runs given in Schroeder, et al., (1980).

As discussed by Schroeder, et al., (1980), accuracy can only be estimated in terms of comparison to "recommended" standard concentrations. Furthermore, accuracy estimates are biased for standards used in calibration. Keeping this in mind, accuracy of calibration and check standard analyses was fairly good except for Cu, Cr, and Co. Table VIII A lists recommended standard concentrations, and table VIII B lists accuracy estimates (in terms of percent deviation from recommended values) for the calibration standards (denoted \*) and check standards. The BR data are from the precision runs listed in table VII. In general, but with some exceptions, deviation from recommended values was greatest at very high and very low concentrations. The range in estimated accuracy of standards with concentrations in the range of NAM samples is given in table VIII B. The accuracy is generally better than 10%, but depends somewhat on concentration. It should be noted that these estimates include all standards with concentrations in the range of NAM samples, and in many cases, most of these standards show much better accuracy. For example, excluding samples with extremely high Cr, the accuracy of standards with concentrations similar to NAM samples is within 10 or 12%, except for BR which was 26% too low. BR

TABLE VII

TRACE ELEMENT PRECISION ESTIMATES BASED ON STANDARD BR

ELEMENT	Zr	Y	Sr	Rb	Zn	Cu*	NI*	Cr	V*	Co	Ba*	Nb
Recomm. concn. (ppm)	250	30	1320	47	150	72	260	380	235	50	1050	100
Mean	296.0	31.3	1306	46	129.5	79	261	281	240	56	1053	126
Std. Dev.	15.9	0.6	15.0	0.4	1.5	1.5	2.1	1.6	4.5	1.6	15.5	2.5
Precision	5.4	1.9	1.1	0.9	1.2	1.9	0.8	0.6	1.9	2.9	1.5	2.0

Notes: Precision defined as percent deviation of the standard deviation from the mean ((std. dev./mean) x 100).

Mean values for Zr, Y, Sr, and Rb are from 10 replicate analyses; values for all other elements are the means of 14 analyses.

\* denotes elements for which BR was used for curve calibration.

TABLE VIII A

## RECOMMENDED STANDARD CONCENTRATIONS

STANDARD	Zr	Y	Sr	Rb	Zn	Cu	Ni	Cr	V	Co	Ba	Nb
AGV-1	225	21*	657*	67*	84	60	18.5*	12.2*	125	14.1*	1208	15*
DTS-1	3		0.3		45*	7	2269	4000	10	133	2.4	
MRG-1			260	8*	185*	135*	200*	420*	520	87	71*	
BCR-1	190*	37*	330*	46.6*	120*	18.4*	16	17.6*	399*	38*	675*	13.5*
GSP-1	500	30*	233*	254	98*	33*	12.5*		53*	6.4	1300	29*
W-1	105*	25*	190*	21*	86*	110*	76*	114*	264*	47*	160*	9.5*
BR	250		1320		150	72*	260*	380	235*	50	1050*	100?
37-332-3-4			87	1								
37-332-35-2	32*		73	3								
8-2								34*				
PCC-1	7				36		2339	2730	30	112*	1.2	
123-5D3												6*

Notes: All values are ppm.

Standards used for curve calibration are denoted \*.

Standard designations are given in Schroeder, et. al. (1980).

TABLE VIII B

## ACCURACY AND DETECTION LIMITS OF TRACE ELEMENTS ANALYSES

STANDARD	Zr	Y	Sr	Rb	Zn	Cu	Ni	Cr	V	Co	Ba	Nb
AGV-1	+9.3	+4.8	0.0	+0.1	-3.3	-15.3	+3.8	-12.3	-2.5	+16.3	-14.4	-0.7
DTS-1					+4.4	-25.7	+6.0	-25.9	+35.0	+2.0		
MKG-1			+2.8	-5.0	+0.4	-4.1	-2.6	-0.1	+3.6	+1.3	+8.3	
BCR-1	+0.2	+1.9	-0.5	-1.1	+0.2	+22.3	-5.0	-11.4	+0.5	-5.3	-0.6	+4.4
GSP-1	+7.1	-7.3	+0.6	-0.5	-0.7	-25.8	-3.2		+5.7	+26.6	-32.8	-0.3
W-1	-0.9	+2.0	0.0	+3.8	-2.7	+1.0	+2.1	+0.3	-2.0	-8.0	-3.3	-4.2
BR	+18.4		-1.1		-13.3	+9.7	+0.4	-26.1	+2.1	+12.0	+0.3	+26.0
332-3-4			+4.7									
332-35-2	+1.6		+3.8	+10.0								
8-2							+10.3					
PCC-1					+25.3			-17.8	+11.0	+0.6		
123-5D3											+10.0	
Estimated <sup>1</sup> Accuracy NAM rocks	+9	+7	+5	+5	+4	+25	+6	+26	+11	+13	+8	+4
Detection <sup>2</sup> Limits	20	16	9	3	15	7*	-12*	12*	18	6*	6*	10

Notes: 1 Range in accuracy of check standards with concentrations similar to NAM samples.

2 Detection limits of samples denoted \* are set at the concentration of the standard with lowest conc. which checked reasonably accurate; all others set at (conc. intercept + 3 s.d. intercept).





TABLE IX (continued)

	720A	733B	751A	764C	777A	800A	905A	909A	910B	963A	979B
Zr	32	20	26		72	26			22	32	23
Y					27					20	
Sr	208	107	171	106	227	175	23	20	201	164	214
Rb											
Zn	24	24	36	19	61	31	28	45	24	38	27
Cu	42	49	65	102	58	199	120	218	35	64	57
Ni	85	95	192	80	139	184	411	569	139	71	137
Cr	193	458	369	341	225	510	2121	3250	1070	333	201
V	72	94	63	110	226	89	133	230	120	205	53
Co	27	39	52	36	55	48	66	75	42	38	40
Ba											
Nb											

Notes: All values are ppm. All samples were analyzed for each element, blank spaces = below detection limit.

tended to deviate significantly for several elements (Zr, Zn, Cr, Nb). A possible reason may be degradation of the pellet surface from continued use.

Cobalt concentrations are probably high due to contamination from the tungsten carbide mixer mill based on a study by J. Dyer (personal communication, 1981) comparing samples prepared in a mixer mill with samples ground in an alumina mortar. She observed no systematic variations in other elements.

Unfortunately, the detection limits of some elements were not as low as desired, because the intercepts of some calibration curves deviated significantly from zero. Detection limits for elements with positive concentration intercepts were taken as the intercept plus 3 times the standard deviation of the intercept (the true intercept should be within 3 standard deviations at the 99% confidence level). For elements with negative concentration intercepts (Cu, Cr, Ba, Nb), the detection limits were set at the concentration of the standard with lowest concentration which checked reasonably accurate. Detection limits are listed in table VIII B.

Deviation of the intercept from zero can be attributed to several factors, including lack of adequate calibration standards, contamination, and improper correction factors. The curve for Y is the best example of the first problem. The concentration intercept is 4.3 ppm and the range in Y concentration among available standards is only 21-37 ppm. Because no standard is available to define the curve at low concentration, a small variation in corrected intensities among the calibration standards may produce a significant variation in slope and thus intercept (Schroeder, written communication to S.E. DeLong, 1978).

Schroeder, et al., (1980) have apparently solved this problem with the addition of a wider range of calibration standards and have improved accuracy and detection limits of Y considerably.

Contamination is another possible cause of intercept deviation. Schroeder (written communication to S.E. DeLong, 1978) stated that large negative concentration intercepts are consistently observed for Cu and Cr and that the problem is probably caused by contamination from the tube target, resulting in large intensity readings at zero concentration. He stated that this should not affect calibration of the curve nor calculation of concentrations (i.e., the curve is simply shifted toward higher intensities). Low concentration standards are available to verify this and therefore detection limits are good (Cu 7 and Cr 12 ppm).

The situation for Ba is similar to Cu and Cr. The curve shows excellent linearity (correlation coefficient = 0.9999) over a large concentration range and to low concentration (6 ppm), but it has a large negative intercept. It is not known if this was due to contamination.

The curves of Zr, Y, Zn, Ni, V, and Co had significant positive concentration intercepts. Some of these curves showed good linearity to concentrations fairly close to the intercept value. For example, the Ni curve, with a correlation coefficient of 0.9996, has an intercept of 8.3 ppm, yet calibration standard GSP-1 (recommended concentration = 12.5 ppm) yields an estimated value of 12.1 ppm. This type problem, where in effect the corrected intensities are zero or negative at low concentrations, are probably due to slight errors in the correction procedures of matrix effects.

### 3.3 Mineral Analyses

Complete major element analyses of plagioclases, clinopyroxenes, and brown hornblendes were performed with the LDGO microprobe. These analyses are presented in tables X A-C. Supplemental semi-quantitative data were obtained with the instrument at State University of New York at Albany, an ETEC with solid state detection system, and are listed in table XIII.

Seven check analyses of the LDGO standard Kakanui Kaersutite were performed during the course of mineral analyses. Pertinent statistical data of these checks are listed in table XI. The mean concentrations of  $\text{TiO}_2$ ,  $\text{FeO}^*$ ,  $\text{SiO}_2$ ,  $\text{K}_2\text{O}$ , and  $\text{Al}_2\text{O}_3$  checked within 2% of the accepted values of the kaersutite. The  $\text{Na}_2\text{O}$  mean was about 6% high. The range in deviation from the accepted values was greater, e.g., as much as 9% low for  $\text{TiO}_2$  and 10% high for  $\text{Na}_2\text{O}$ .  $\text{K}_2\text{O}$ ,  $\text{Na}_2\text{O}$ ,  $\text{MgO}$ , and  $\text{Al}_2\text{O}_3$  were consistently high while  $\text{CaO}$  consistently checked low. The accuracy and precision should be approximately within the range of percent deviations for samples with concentrations similar to the kaersutite. No estimate of accuracy for  $\text{P}_2\text{O}_5$  and  $\text{Cr}_2\text{O}_3$  is possible because no standard values are known for the Kakanui Kaersutite.

Complete olivine analyses determined with the SUNYA probe for four NAM samples are listed in table XII. No independent checks on the  $\text{FeO}^*$  accuracy were made, but a check on synthetic forsterite standard showed  $\text{MgO}$  and  $\text{SiO}_2$  accuracy was very good.  $\text{CaO}$  was detected in only a few of the points. The standard deviations show the concentrations to be very constant within samples. A one percent change in Fo of a large olivine in sample 635 was observed. A much smaller degree of normal zoning was detected in an olivine of sample 800, but this was less than one

TABLE X-A

PLAGIOCLASE COMPOSITIONS OF SELECTED NAM PLUTONIC ROCKS  
(LDGO MICROPROBE)

SAMPLE	635A	709A	720A	751A	800A	909A
ROCK TYPE	TROC	OG	OG	OG	OG	LHERZ
NUMBER OF POINTS	5	5	5	6	4	4
SiO <sub>2</sub>	48.96	49.88	49.26	48.98	49.20	49.04
TiO <sub>2</sub>	0.07	0.01	0.00	0.00	0.05	0.08
Al <sub>2</sub> O <sub>3</sub>	31.50	32.05	31.46	32.43	31.80	32.02
FeO*	0.33	0.16	0.30	0.30	0.29	0.21
MnO	0.00	0.01	0.04	0.02	0.03	0.03
MgO	0.04	0.00	0.04	0.03	0.03	0.04
CaO	15.85	15.38	15.06	15.57	15.24	15.51
Na <sub>2</sub> O	2.80	2.85	3.13	2.73	2.99	2.95
K <sub>2</sub> O	0.09	0.12	0.11	0.12	0.12	0.11
TOTAL	99.64	100.46	99.40	100.18	99.75	99.99
Ca/(Ca+Na)	0.76	0.75	0.73	0.76	0.74	0.74

TABLE X-B

## CLINOPYROXENE COMPOSITIONS OF SELECTED NAM PLUTONIC ROCKS

(LDGO MICROPROBE)

SAMPLE	635A	709A	720A	751A	800A	909A
NUMBER OF POINTS	3	2	3	5	6	3
SiO <sub>2</sub>	51.71	52.34	50.48	49.97	50.83	51.57
TiO <sub>2</sub>	1.05	0.51	1.22	1.05	1.02	0.51
Cr <sub>2</sub> O <sub>3</sub>	0.26	0.35	0.21	0.21	0.44	0.96
Al <sub>2</sub> O <sub>3</sub>	3.06	2.73	3.67	3.63	3.41	3.47
FeO*	7.05	7.57	7.43	6.57	7.31	6.28
MnO	0.26	0.21	0.28	0.22	0.23	0.22
MgO	15.36	15.00	15.23	15.74	15.00	15.53
CaO	21.05	20.41	21.40	21.06	20.44	21.51
Na <sub>2</sub> O	0.49	0.45	0.55	0.57	0.58	0.58
K <sub>2</sub> O	0.06	0.06	0.08	0.07	0.06	0.06
TOTAL	100.35	99.63	100.55	99.10	99.32	100.69
Mg/(Mg+Fe)	0.80	0.78	0.78	0.81	0.79	0.82

TABLE X-C

## HORNBLLENDE COMPOSITIONS OF SELECTED NAM PLUTONIC ROCKS

SAMPLE	635A	720A	751A	800A
NUMBER OF POINTS	2	4	5	5
SiO <sub>2</sub>	42.79	41.77	42.00	41.96
TiO <sub>2</sub>	3.13	4.51	4.49	4.61
Cr <sub>2</sub> O <sub>3</sub>	0.14	0.27	0.53	0.55
Al <sub>2</sub> O <sub>3</sub>	12.29	12.20	12.07	12.05
FeO*	9.86	10.99	9.16	9.87
MnO	0.10	0.09	0.13	0.13
MgO	15.03	13.78	14.21	14.04
CaO	11.71	11.65	11.53	11.39
Na <sub>2</sub> O	2.90	3.23	3.18	3.28
K <sub>2</sub> O	0.32	0.35	0.37	0.32
TOTAL	98.24	98.84	97.68	98.20
Mg/(Mg+Fe)	0.73	0.69	0.73	0.72

Notes: All analyses performed with LDGO microprobe. Values are the means of the number of points indicated. Sample 800A included a 3 point traverse from rim to core on a single crystal; each point was on different crystals in all other samples.



TABLE XI

ESTIMATED ACCURACY OF LDGO MINERAL ANALYSES BASED ON  
KAKANUI KAERSUTITE STANDARD CHECKS

OXIDE	RECOMMENDED CONC.	MEAN	STD. DEV.	% DEV. MEAN
SiO <sub>2</sub>	40.20	40.40	0.34	+0.5
TiO <sub>2</sub>	5.00	4.92	0.31	-1.6
Al <sub>2</sub> O <sub>3</sub>	13.95	14.14	0.12	+1.4
FeO*	11.06	10.92	0.23	-1.3
MnO	0.09	0.12	0.03	+31.7
MgO	12.87	12.42	0.31	-3.5
CaO	10.20	9.96	0.12	-2.3
Na <sub>2</sub> O	2.54	2.69	0.10	+5.9
K <sub>2</sub> O	2.12	2.16	0.03	+1.7
TOTAL	98.03	97.73		
FeO*/MgO	0.86	0.88		+2.3

Notes: Estimated accuracy at the concentration levels of the kaersutite standard is defined as the percent deviation of the means from the recommended values ((mean-std. conc.)/std. conc.) x 100.

TABLE XII

## OLIVINE COMPOSITIONS DETERMINED WITH SUNYA PROBE

SAMPLE	635A	751A	800A	909A
ROCK TYPE	TROC	OG	OG	LHERZ
NUMBER OF POINTS	7 <sup>a</sup>	8 <sup>b</sup>	10 <sup>c</sup>	6 <sup>d</sup>
SiO <sub>2</sub>	37.98 $\pm$ 0.20	38.63 $\pm$ 0.18	37.91 $\pm$ 0.14	38.85 $\pm$ 0.30
FeO*	20.93 $\pm$ 0.12	19.52 $\pm$ 0.21	21.16 $\pm$ 0.31	17.72 $\pm$ 0.19
MnO	0.31 $\pm$ 0.06	0.32 $\pm$ 0.04	0.29 $\pm$ 0.04	0.29 $\pm$ 0.04
MgO	40.41 $\pm$ 0.28	41.83 $\pm$ 0.25	40.04 $\pm$ 0.34	43.13 $\pm$ 0.30
CaO	0.03	0.05	0.05	0.00
TOTAL	99.66	100.35	99.45	99.99
Fo	77.5	79	77	81
(FeO*/MgO) <sub>liq</sub> <sup>e</sup>	1.73	1.56	1.76	1.37

Notes: a Includes a 4 point traverse across a single crystal; Fo rim = 77, Fo core = 78.

b Includes 3 points on one crystal; total of 6 crystals.

c Includes 3 points on core and 4 points on rim of a single crystal, all with Fo = 77; total of 4 crystals.

d All points on 2 crystals.

e Calculated assuming  $K_{\text{FeO}^*/\text{MgO}}^{\text{ol/liq}} = 0.30$ .

Rock types: TROC - troctolite; OG - olivine gabbro; LHERZ - lherzolite.

Standard deviations are listed for SiO<sub>2</sub>, FeO\*, MnO, MgO.

TABLE XIII

 SEMI-QUANTITATIVE MINERAL CHEMISTRY  
 (SUNYA MICROPROBE)

SAMPLE	205C	630A	635A	709A	720A	751A
ROCK TYPE	OG	OG	TROC	OG	OG	OG
OLIVINE						
Fo	74	72	78	79	76	79
FeO*/MgO*	0.64	0.70	0.51	0.48	0.58	0.47
(FeO*/MgO) <sup>1</sup> <sub>liq</sub>	2.13	2.32	1.73	1.59	1.92	1.56
CLINOPYROXENE						
Mg/(Mg+Fe)	0.80	0.78				0.82
FeO*/MgO	0.45	0.49				0.38
K <sub>D</sub> <sup>2</sup> <sub>pyx/liq</sub>	0.21	0.21				0.24
ORTHOPYROXENE						
Mg/(Mg+Fe)		0.76				
FeO*/MgO		0.58				
K <sub>D</sub> <sup>2</sup> <sub>pyx/liq</sub>		0.25				
PLAGIOCLASE						
Ca/(Ca+Na)	0.61	0.66				

TABLE XIII (continued)

SAMPLE	800A	909A	910B	979B	777A
ROCK TYPE	OG	LHERZ	OG	OG	Hb-OG
OLIVINE					
Fo	77	81		77	62
FeO*/MgO	0.54	0.41		0.54	1.08
(FeO*/MgO) <sub>liq</sub> <sup>1</sup>	1.77	1.37		1.78	3.59
CLINOPYROXENE					
Mg/(Mg+Fe)	0.80	0.84	0.78	0.80	0.71
FeO*/MgO	0.46	0.33	0.48	0.43	0.75
K <sub>D</sub> <sup>1</sup> <sub>pyx/liq</sub>	0.26	0.24		0.24	0.21
ORTHOPIYROXENE					
Mg/(Mg+Fe)		0.82		0.79	
FeO*/MgO		0.39		0.47	
K <sub>D</sub> <sup>1</sup> <sub>pyx/liq</sub>		0.28		0.26	
PLAGIOCLASE					
Ca/(Ca+Na)	0.74	0.74	0.73	0.78	0.60

Notes: 1 Calculated assuming  $K_{\text{FeO}^*/\text{MgO}}^{\text{ol/liq}} = 0.30$ .

Rock types: OG - olivine gabbro; TROC - troctolite;  
LHERZ - lherzolite; Hb-OG - hornblende-olivine gabbro.

percent Fo. The slightly larger standard deviation in FeO\* of sample 800 was due to inclusion of one analysis of a slightly dusky crystal (iddingsite?) which had Fo<sub>78</sub>. The other 9 points of this sample all had Fo<sub>77</sub>.

Attempts to analyze olivine with the LDGO probe produced consistently high totals (102-103%). MgO values were similar for both probes, but FeO\* values were 1-2 wt.% higher on the LDGO probe. SiO<sub>2</sub> also ran 0.5-1.0 wt.% high. The problem occurred even though two different MgO standards were used at LDGO.

The FeO\*/MgO ratios of clinopyroxenes determined with the SUNYA probe were consistently lower than values obtained with the LDGO probe for the same samples. The FeO\*/MgO ratios of olivines and pyroxenes determined with the SUNYA probe were very consistent over a wide range of operating conditions. For example, olivines in sample 909A were used as a check standard whenever olivine or pyroxenes were analyzed and the Fo content always checked as 81 or 82.

It is therefore cautioned that comparisons based on FeO\*/MgO should not be made between the two sets of data. To maintain internal consistency, the SUNYA data are used in discussions concerning FeO\*/MgO in this thesis. This choice is based on importance of and availability of olivine data, and also the determination of orthopyroxene FeO\*/MgO with the SUNYA probe.

The molecular proportions of Ca/(Ca+Na) were determined for plagioclases as a measure of fractionation in lieu of An content because accurate K<sub>2</sub>O concentrations were not obtained with the SUNYA probe. This proportion is denoted Ca<sup>#</sup> in this study. Ca<sup>#</sup> was determined with both microprobes for plagioclases of samples 800 and 909 and were

the same. Therefore comparisons of this parameter between samples analyzed with either instrument are probably acceptable.

Selected chemical parameters are plotted in figure 4. Ca-Mg-Fe proportions in clinopyroxenes and hornblendes were analyzed with the LDGO probe. Ca values for orthopyroxenes are not included in the diagram, but were less than 2 wt.%.

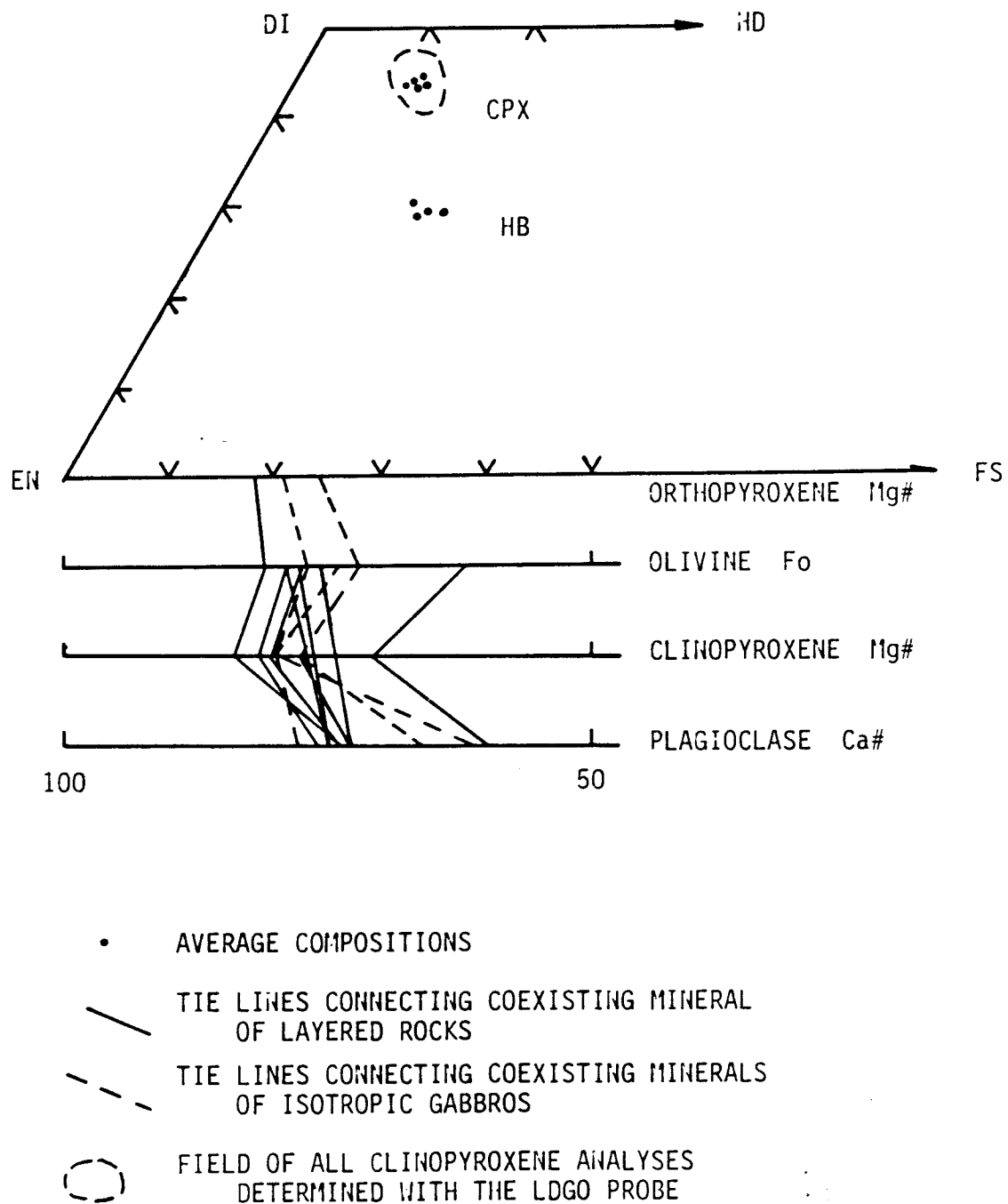


Figure 4. Selected chemical features of minerals of NAM plutonic rocks. Ca-Mg-Fe proportions in clinopyroxenes and hornblendes were determined with the LDGO microprobe. Mg/(Mg+Fe) of olivines and pyroxenes were determined with the SUNYA probe. Ca/(Ca+Na) of plagioclases were determined with either probe. Ca values of orthopyroxenes are not included in the diagram, but all were less than 2.

## CHAPTER IV

### DISCUSSION OF CHEMICAL OBSERVATIONS

#### 4.1 CHEMICAL CLASSIFICATION OF BAY OF ISLANDS MAGMA

Irvine and Findlay (1972) first suggested the Bay of Islands magma was of "low silica activity" based on the scarcity of orthopyroxene in the plutonic rocks and the fact that they are commonly nepheline rather than hypersthene normative. They also noted the gabbros were poor in  $K_2O$  and  $TiO_2$ , like ocean ridge basalts. From these observations, they suggested the magma might have been similar to "transitional tholeiite" or mildly alkaline magmas found, for example, along the mid-Atlantic Ridge.

Riccio (1976) noted that  $TiO_2$  in lavas and dike rocks increased with increasing  $FeO^*/MgO$  in a manner similar to tholeiitic trends. He observed this same relationship in clinopyroxenes of plutonic rocks, while aluminum varied inversely with  $FeO^*/MgO$ . He also observed that Ca-Mg-Fe proportions in the plutonic clinopyroxenes were between those crystallized from alkalic and tholeiitic liquids. Riccio also concluded the Bay of Islands magma was mildly alkaline or a transitional tholeiite.

Malpas (1978) reached the same conclusion based on the following observations: 1) REE abundances and patterns of lava and dike rocks are similar to mid-Atlantic Ridge basalts (see also Suen, et al., 1979), 2) most clinopyroxenes of the plutonic rocks have titanium and aluminum concentrations consistent with tholeiites, based on Kushiro's



(1960) classification, 3) Bay of Islands rocks follow an iron enrichment trend on an AFM diagram, 4) most lavas and dikes plot on the tholeiitic side of the MacDonald and Katsura (1964) boundary on an alkalies versus silica diagram, while several plot on the alkaline side, 5) normative compositions of the lavas and dikes plot on both sides of the critical plane of undersaturation in the simplified normative basalt tetrahedron of Yoder and Tilley (1962).

I do not believe the studies cited above have definitely established the presence of alkaline tendency of the Bay of Islands magma. I believe alteration in the lavas and dikes may be responsible for the apparent alkaline nature seen in the norms and on the silica versus alkalies diagram. The lava and dike rocks on Malpas' (1978) silica versus alkalies diagram show no apparent coherent trend but tend toward a sub-vertical scatter, especially the lavas, across the alkaline-subalkaline boundary. Malpas himself attributed this partly to sodium metasomatic alternation and stated that the samples with highest alkali content were the most altered. Interestingly, only three samples analyzed in this thesis were nepheline normative. All were plutonic rocks and two of the three, samples 633 and 720, showed the most petrographic evidence of alteration.

Whole rock major element compositions of basalt 104 and diabase 109 are compared with representative compositions of ocean floor basalts and other selected samples in table XIV. In general, the Bay of Islands samples are most similar to the ocean floor tholeiites and Tortuga dikes. The major differences are the high  $\text{Na}_2\text{O}$  and low  $\text{CaO}$  of the Bay of Islands samples. Both the sense and degree of variation

TABLE XIV

## ANALYSES OF SELECTED OCEAN-FLOOR AND RELATED ROCKS

	NAM 104C	NAM 109C	1	2	3	4	5	6	7	8
SiO <sub>2</sub>	50.51	48.12	46.8	49.56	49.21	49.46	48.21	41.71	51.54	49.90
TiO <sub>2</sub>	1.93	1.40	1.8	0.96	1.31	1.27	1.60	2.07	1.13	1.10
Al <sub>2</sub> O <sub>3</sub>	15.28	17.04	14.9	15.50	15.81	15.83	16.17	16.33	13.76	13.70
FeO*	10.80	9.46	9.5	9.26	9.16	10.67	9.80	9.91	11.28	11.99
MnO	0.24	0.25	0.1	0.18	0.16	0.16	0.18	0.19	0.18	0.20
MgO	7.25	8.21	5.5	7.32	8.53	7.96	7.34	8.44	6.09	6.85
CaO	5.59	8.55	10.2	9.35	11.14	11.04	12.16	10.53	10.23	6.23
Na <sub>2</sub> O	4.36	2.97	4.4	3.22	2.71	2.25	2.51	2.72	2.33	3.20
K <sub>2</sub> O	0.34	0.52	0.3	0.83	0.16	0.42	0.35	0.65	0.62	2.22
P <sub>2</sub> O <sub>5</sub>	n.d.	0.19	0.2	0.08	0.15	0.18	0.25	0.51	0.13	0.12
TOTAL	100.00	100.00	98.4	98.23	98.34	99.24	100.03	99.67	99.08	97.22
FeO*/MgO	1.49	1.15	1.7	1.26	1.07	1.34	1.34	1.17	1.85	1.75
Zr	138	98	138	87	95	85	100	165	---	---

## SOURCES OF ANALYSES IN TABLE XIV

ANALYSIS	SOURCE
104C, 109C	This study.
1	NAM pillow lava - average of core and selvage of a pillow from NAM; Williams and Malpas, 1972.
2	NAM diabase - average of 3 diabase dikes from NAM; Suen, et. al., 1979.
3	Average abyssal tholeiite - Reported in Strong, 1974; compiled from Engle, A.E.J., C. Engle, and T. Havens, <u>Geol. Soc. Amer. Bull.</u> , 76, 1965; and Melson, W.G., G. Thompson, and T. VanAndel, <u>J.G.R.</u> , 73, 1978.
4	Average of 20 Tortuga ophiolite sheeted dikes; Stern, 1979.
5	LIL enriched tholeiite- sample 11-102, MAR 43°N; Shibata, T., G. Thompson, and Frey, 1979.
6	Alkali basalt - sample 5-6, MAR 43°N; Shibata, T., G. Thompson, and F.A. Frey, 1979.
7	Fresh Deccan tholeiite; Vallance, T.G., 1974.
8	Spilitized Deccan tholeiite - Vallance, T.G., 1974.

are consistent with alteration effects observed in ocean tholeiites (Hart, et al., 1974), spilitization of Deccan flow tholeiites (Vallance, 1974) and alteration of ophiolite pillow basalts (Seguin and Laurent, 1975; Coish, 1977). Furthermore, the very low CaO of basalt 104C is not consistent with any reasonable magma type in this range of SiO<sub>2</sub> and FeO\*/MgO. Stable trace elements of the NAM samples are also similar to ocean floor tholeiites, while mobile trace elements are quite different. Basalt 104 does plot slightly in the alkaline field on the alkalis versus silica diagram, while diabase 109 plots in the sub-alkalic field. Neither sample has normative nepheline like some of Malpas' (1978) samples, but then these two samples were chosen for analysis because they appeared less altered than other available NAM basalts and diabases.

The observation by Irvine and Findlay (1972) that Bay of Islands gabbros had low TiO<sub>2</sub> and K<sub>2</sub>O concentrations led them to suggest a similarity to LIL depleted ocean floor tholeiites. However, this feature may more readily be explained by the incompatible nature of these elements and their consequent exclusion from the plutonic rocks, if indeed these rocks formed in the manner described in chapter 2.

Finally, Malpas' (1978) demonstration of an iron-enrichment trend involves the combination of plutonic rocks with lavas and dikes on an AFM diagram. As discussed previously and as pointed out by Church and Riccio (1977), plutonic rocks do not represent liquid compositions and cannot therefore be used to indicate liquid trends. No discernible trend occurs among the basalts and diabases on Malpas' AFM plot.

Most of the other observations cited by these authors support the contention that the Bay of Islands magma was tholeiitic and possibly typical ocean floor tholeiite. The flat to slightly depleted LREE

patterns of basalts and diabase dikes (Malpas, 1978; Suen, et al., 1979) are especially inconsistent with alkaline tendencies, but are less depleted than highly depleted abyssal tholeiites. This may indicate that these rocks are transitional between LIL depleted and enriched abyssal tholeiites. The stable LIL elements of basalt 104C and diabase 109C are in the range of overlap between depleted and enriched tholeiites at their respective  $\text{FeO}^*/\text{MgO}$ , and therefore are not diagnostic.

Chemical data presented in this study are not well suited to magma classification because only two samples representing probable near liquid compositions, basalt 104 and diabase dike 109, were analyzed. Nevertheless, all applicable classification schemes suggest these samples are tholeiitic, with the exception of basalt 104 on the silica versus alkalis diagram discussed in the previous section.

In terms of major elements, both samples plot in the tholeiitic fields on diagrams defined by Miyashiro (1973, 1975) based on  $\text{SiO}_2$ ,  $\text{FeO}^*$ ,  $\text{MgO}$ , and  $\text{TiO}_2$ . Furthermore, the two samples follow the average abyssal tholeiite trends on the  $\text{FeO}^* - \text{FeO}^*/\text{MgO}$  and  $\text{TiO}_2 - \text{FeO}^*/\text{MgO}$  diagrams. Riccio (1977) also noted this characteristic. The two samples straddle the abyssal tholeiite trend (Miyashiro, 1973) on the  $\text{SiO}_2 - \text{FeO}^*/\text{MgO}$  diagram. Although  $\text{SiO}_2$  may be affected by alteration,  $\text{TiO}_2$ ,  $\text{FeO}^*$ , and  $\text{FeO}^*/\text{MgO}$  are less affected (Miyashiro, 1975; Winchester and Floyd, 1976) and thus are probably fairly reliable.

Nevertheless, in view of the susceptibility to alteration of many of the major elements, and considering the probable degree of alteration of Bay of Islands extrusive and hypabyssal rocks, it seems wise to rely more heavily on discriminant stable trace elements or isotopes. As mentioned, the REE data of Malpas (1978) provide evidence of an abyssal tholeiitic magma. Jacobsen and Wasserburg (1979)

found the presumed stable  $\text{Nd}^{143}/\text{Nd}^{144}$  of Bay of Islands clinopyroxenes to be similar to the distinctive ratios of MORB.

Both the basalt and diabase of this study plot in the ocean floor basalt fields on the Ti-Zr and Ti-Zr-Y diagrams proposed by Pearce and Cann (1973), and on the Ti-Y/Nb diagram of Floyd and Winchester (1975). Only diabase 109 was analyzed for  $\text{P}_2\text{O}_5$ , and this sample appears sub-alkaline on all the  $\text{TiO}_2$ , Zr,  $\text{P}_2\text{O}_5$ , Y, Nb diagrams of Floyd and Winchester. However, the Y/Nb ratios are very uncertain due to the very low concentration and analytical uncertainty of Nb, especially for the basalt. Additionally, the NAM pillow lava analyzed by Williams and Malpas (1972) has  $\text{TiO}_2$ ,  $\text{P}_2\text{O}_5$  and Zr concentrations consistent with a sub-alkaline magma. The Ti-Zr-Sr diagram of Pearce and Cann (1973) was not used due to the mobility of Sr.

In view of this chemical data, I believe the Bay of Islands magma was tholeiitic and consistent with typical LIL depleted ocean floor tholeiite. This is consistent with the geological evidence that the Bay of Islands ophiolite probably formed at a mid-ocean spreading center, although chemically a small ocean basin is not ruled out. The alkaline tendency of the magma has not, I believe, been proven.

#### 4.2 ESTIMATION OF PROPORTION OF TRAPPED LIQUID/PRIMOCRYSTS IN NAM ADCUMULUS TEXTURED ROCKS

One use of whole rock chemistry of plutonic rocks is calculation of the amount of trapped liquid. Stern (1979) has described this method and has used it in conjunction with REE data to model the relationship between gabbros and extrusive rocks of Chilean ophiolites. The method

is to determine from mineral chemistry the  $\text{FeO}^*/\text{MgO}$  of the liquids presumed in equilibrium with the plutonic rocks, and ratio the whole-rock concentration of incompatible elements (e.g., Zr) to basalts or diabases of equal  $\text{FeO}^*/\text{MgO}$ .

This method is based on several assumptions. First, it assumes that the plutonic rocks crystallized from the same liquid as did the lavas and dikes. Students of ophiolites generally believe this to be true based on geologic and geochemical evidence. For example, the lack of intrusive contacts in the plutonic rocks of NAM and the gradational change in texture between adcumulus and orthocumulus textured rocks support the existence of a single, large magma chamber rather than multiple chambers, and the presence of "rootless" diabase dikes extending only part way into the gabbros (i.e., the lack of feeder conduits) suggest the extrusive rocks and plutonic rocks formed from the same magma. Other workers have interpreted chemical data to support the consanguinous relationship between the extrusive and plutonic members of various ophiolites. For example, Pallister and Knight (1981) and Stern (1979) supported this conclusion for the south Oman and Chileau ophiolites, respectively, based on REE and other trace elements. On the other hand, some investigators believe trace element data for some ocean-floor rocks indicates the presence of multiple liquids (e.g., Langmuir, et al., 1978).

A second assumption is that the incompatible elements and  $\text{FeO}^*/\text{MgO}$  follow a single, well-defined variation trend. This has been found to be the case in many ocean floor and ophiolite suites, although, again the presence of multiple liquids with different trace element characteristics would preclude use of this method. A single, well-defined trend between Zr and  $\text{FeO}^*/\text{MgO}$  has been documented for the Tortuga ophiolite (Stern,

1979), and Elthon (personal communication) has calculated the percent trapped liquid to be about 5% in Tortuga adcumulates and 20-40% in orthocumulates.

An important limitation of this method is that it assumes that the incompatible elements reside solely in phases crystallized from trapped liquid, and therefore this method yields maximum estimates. The partition coefficient data of Pearce and Norry (1979) indicate that significant amounts of the "incompatible" elements Ti, Zr, Y, Nb may be contained in certain minerals, and wide variations in proportions of primocrysts can introduce considerable error into these estimates.

In spite of these limitations, this method can indicate significant differences in the amounts of trapped liquid if care is exercised. Also, if the plutonic rocks are fresh enough that accurate modal abundances of original igneous minerals can be determined, estimates of percent pore liquid can be corrected for the amount of incompatible elements in the primocrysts, using either partition coefficients or mineral compositions.

Results of these computations for several NAM plutonic rocks are listed in table XV. Unfortunately, use of this method was limited for several reasons. First, only two samples from this study and three diabases from Suen, et al., (1979) are available to establish the relationship between Zr and  $\text{FeO}^*/\text{MgO}$  in the liquid. Nevertheless, 4 of these 5 samples plot nearly on a straight line with a slope parallel to that of Tortuga lavas and dikes (Stern, 1979). Also, a 10% variation in projected Zr for any  $\text{FeO}^*/\text{MgO}$  of the liquid results in a maximum variation of  $\pm 2\%$  calculated pore volume. Second, the incompatible element concentrations of many of these NAM plutonic rocks were below the limits of detection, due to a combination of analytical limitations,



TABLE XV

## ESTIMATED PERCENTAGES OF TRAPPED LIQUID IN NAM PLUTONIC ROCKS

SAMPLES	CALIB. SAMPLES		NAM PLUTONIC ROCKS		
	104C	109C	205C	635A	709A
CALIBRATION PARAMETERS					
$(\text{FeO}^*/\text{MgO})_{\text{liq}}^1$	1.49	1.15	2.13	1.73	1.59
whole-rock Zr (ppm)	139	98	32	27	bd1
whole-rock $\text{TiO}_2$ (wt.%)	1.93	1.44		0.14	0.18
projected $\text{Zr}^2$			222	167	
bulk $K_{\text{Zr}}^{\text{min/liq}^3}$				0.012	
bulk $K_{\text{Ti}}^{\text{min/liq}^3}$				0.045	0.087
PORE LIQUID ESTIMATES					
from Zr			14.2	16.3	
from Zr adjusted for bulk $K_{\text{Zr}}$				15.0	
from Ti mineral comp. and modes				5.2	
from Ti and bulk $K_{\text{Ti}}$				1.6	-0.1

TABLE XV (continued)

SAMPLES	NAM PLUTONIC ROCKS				
	720A	751A	777A	800A	909A
CALIBRATION PARAMETERS					
$(\text{FeO}^*/\text{MgO})_{\text{liq}}$ <sup>1</sup>	1.92	1.56	3.59	1.77	1.37
whole-rock Zr	32	26	72	26	bdl
whole-rock $\text{TiO}_2$				0.29	0.35
projected Zr <sup>2</sup>	190	147	389	172	
bulk $K_{\text{Zr}}$ min/liq <sup>3</sup>				0.032	0.070
bulk $K_{\text{Ti}}$ min/liq <sup>3</sup>				0.103	0.212
PORE LIQUID ESTIMATES					
from Zr	16.6	17.9	18.4	14.8	
from Zr adjusted for bulk $K_{\text{Zr}}$				11.6	
from Ti mineral comp. and modes				2.1	-0.6
from Ti and bulk $K_{\text{Ti}}$				1.9	-1.1

## Notes:

- 1 Calculated assuming  $K_{\text{FeO}^*/\text{MgO}}^{\text{ol/liq}} = 0.30$ .
- 2 Concentration of Zr in liquids from which plutonic rocks crystallized is projected from the Zr vs.  $\text{FeO}^*/\text{MgO}$  relationship of basalt 104C and diabase 109C.
- 3 Bulk rock distribution coefficients are calculated from mineral modes and the mineral distribution coefficients recommended by Pearce and Norry (1979) for basic magmas ( $\text{SiO}_2 = 50\%$ ).

bdl - below detection limit.

and the probable adcumulus nature of these rocks. I've used Zr and Ti for these calculations because data is available for the largest number of samples. Zircon has not been seen in these rocks, and Fe-Ti oxides are minor (less than 0.5%). Third, modal determinations are not available for some samples due to alteration. Fourth, mineral compositions are available for a limited number of samples.

Table XV lists percent pore liquid calculated in several ways, including adjustments made for modal volumes and either mineral analyses or distribution coefficients. Problems with these methods, as evidenced by calculated negative pore volumes and discrepancies among the methods, are likely due to inaccuracy in analytical data, inaccuracy and variability in distribution coefficients, variance of Ti mineral analyses from average compositions, variations in the liquid content of various elements, and modal inaccuracy due to fine scale layering.

All of the samples in table XV are adcumulus or possibly mesocumulus textured. No orthocumulates from NAM were included because mineral chemistry is not available to determine the equilibrium liquid  $FeO^*/MgO$ . The Zr values determined here are higher than Elthon (1981) determined for Tortuga adcumulates (about 5% trapped liquid) but less than his orthocumulate samples (20-40% trapped liquid). At present, it is not possible to determine if the difference is real or due to a lack of a good liquid Zr -  $FeO^*/MgO$  curve for the NAM lavas and dikes. It was noted that some chemical zoning occurs in clinopyroxenes and plagioclases of some of these samples, that is, they may be classified as mesocumulates rather than strict adcumulates. This is in accord with the trapped liquid estimates being between 10-20%. By definition (Wager, et al., 1960), adcumulates have less than 5% trapped liquid.

Elthon (personal communication) and Pallister and Hopson (1981) reported observing no zoning in true adcumulus textured rocks in the Tortuga and S. Oman ophiolites, respectively.

The intermediate pore liquid values and mild zoning suggest the NAM samples in this study area may have undergone a cooling history intermediate between slow cooled adcumulates and rapidly cooled orthocumulates. Perhaps this is related to the unique location of these samples near where the crust thinned. The increased thickness of isotropic gabbros may also be related to a faster cooling rate extending deeper into the chamber, possibly due to decreased input of magma. McBirney and Noyes (1979) suggested fine scale igneous layering would not develop where cooling rate is high.

#### 4.3 MINERAL ACCUMULATION VS. IN SITU CRYSTALLIZATION

The long accepted theory that most layered plutonic rocks formed by gravitational accumulation and sorting of crystals (Wager and Deer, 1939; Wager et al., 1960) has been seriously questioned recently (Campbell, 1978; McBirney and Noyes, 1979; Casey, 1980) based on field observations, theoretical considerations, and chemical data. Some of the features not easily explained by the "cumulus theory" include: 1) certain poikilitic textures, 2) perpendicular growth features (e.g., comb structures, harrisitic olivines, crescumulate layering), 3) gradation of compositional igneous layering from low to near vertical primary dip (e.g., in the Jimberlana intrusion, Campbell, 1978), 4) presence of presumed buoyant plagioclase at the bottom of magma chambers and dense phases in roof rocks, 5) efficient layer separation of phases of similar density and size, 6) regular trace element chemical variations within modally graded

layered rocks, and 7) the large nucleation activation energy required for homogeneous nucleation energy in large magma chambers compared to heterogeneous or self-nucleation energies required near the chamber margins. Detailed discussion of the arguments can be found in these papers and references cited therein. The mineral chemical data presented here support Casey's (1980) interpretation that in situ crystallization was the primary mechanism operating in the NAM magma chamber.

One of the arguments favoring in situ crystallization is the preponderance of equilibrium mineral assemblages in the layered plutonic rocks of ophiolites and some stratiform continental intrusions. Based on the hydraulic inequivalency in size and density of mineral assemblages in ophiolites and layered continental intrusions, most geologists believe that if physical accumulation of crystals occurs, it must be by nucleation and settling from widely varying depths of the magma chamber or by deposition through current action (e.g., Jackson, 1961; Wager and Brown, 1968). At any rate, each of these mechanisms would be expected to bring together crystals formed in different parts of the magma chamber. Unless the magma body was chemically very homogeneous, the crystals in the resulting rocks would not likely be in chemical equilibrium with each other. This is especially true in closed system intrusions in which progressive fractionation of the liquid produces a wide range of mineral compositions, yet studies of the Skaergaard (McBirney and Noyes, 1979) and several ophiolites, e.g., Oman (Pallister and Hopson, 1981; Smewing, 1981), Tortuga and Sarmiento (Stern, 1979) and Bay of Islands (Church and Riccio, 1977) show that minerals in the plutonic accumulates are generally in equilibrium.

It was found that olivines within any NAM plutonic sample analyzed in this study have a maximum variation of one percent Fo. This consistency in composition held even between widely differently sized crystals. Because size has the greatest effect on settling rate, large and small crystals within a rock should have settled from different depths in the magma chamber. Noting the definite though moderate variation in olivine composition with stratigraphic height in the plutonic complex, the magma composition must vary somewhat with depth, and crystals settling from different depths should reflect this.

Ca<sup>#</sup> of plagioclases and Mg<sup>#</sup> of clinopyroxenes are somewhat more variable, with the former varying by as much as 4 units and the latter by up to 6 units within individual samples. Much of these ranges have been observed within single zoned crystals. This variability is attributed to in situ fractionation of the liquid. Some re-equilibration may have occurred, especially in olivines. I believe this is a more likely explanation than settling from various parts of the chamber based mainly on the constant olivine compositions and the notable stability of  $K_D^{OL/L} \text{FeO}^*/\text{MgO}$ . Furthermore, settling should be reversed if settling occurred (see section 4.4), but is always normal.

The apparent  $K_D^{CPX/L}$  in each of the three ophiolites is approximately 0.24, based on an assumed  $K_D^{OL/L} = 0.30$  (Roeder and Emslie, 1970). Figure 5 shows coexisting NAM olivine and clinopyroxene  $\text{FeO}^*/\text{MgO}$ <sup>1</sup> plotted against  $\text{FeO}^*/\text{MgO}$  of equilibrium liquids calculated from  $\text{FeO}^*/\text{MgO}$  of olivines using  $K_D^{OL/L} = 0.30$  (after Church and Riccio, 1977). The

---

<sup>1</sup> Data obtained with LDGO microprobe excluded due to possible systematic error in  $\text{FeO}^*$ . See section 3.3 for discussion.

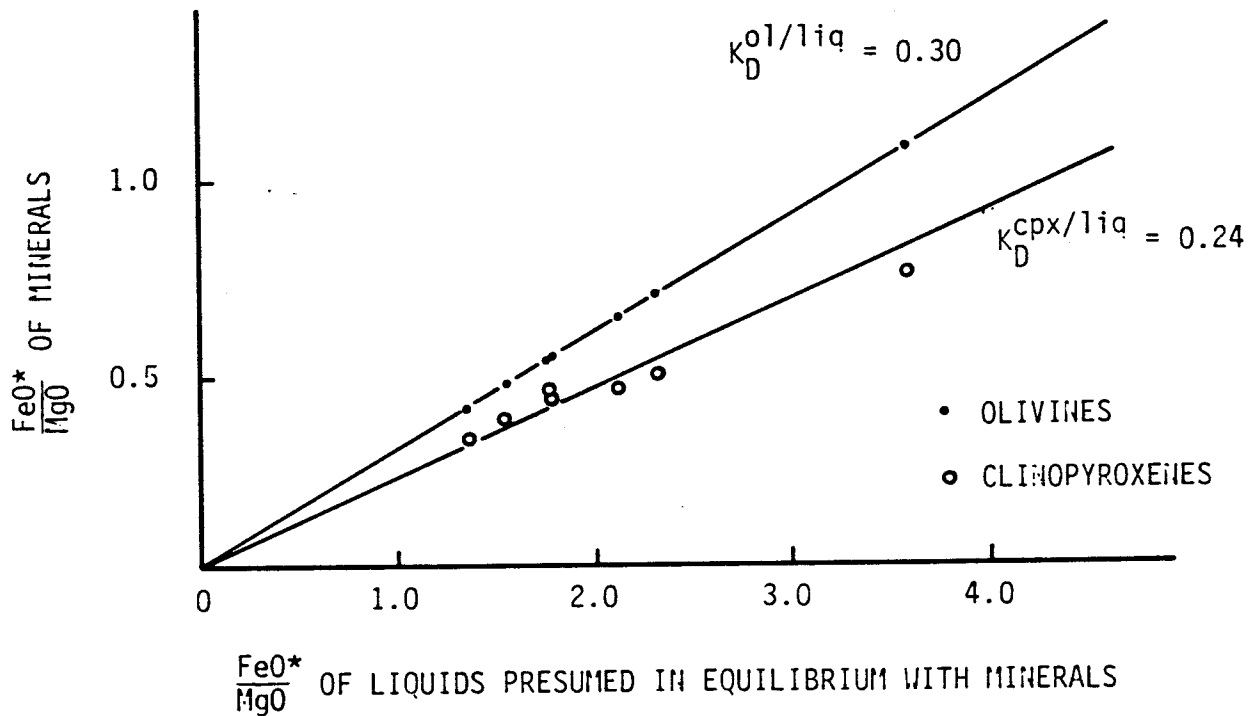


Figure 5.  $\text{FeO}^*/\text{MgO}$  of coexisting olivines and clinopyroxenes of North Arm Mountain plutonic rocks versus  $\text{FeO}^*/\text{MgO}$  of liquids presumed in equilibrium with these minerals.  $\text{FeO}^*/\text{MgO}$  of liquids were calculated assuming  $K_D^{\text{ol/liq}} = 0.30$ .

clinopyroxene data, although scattered, fit an average  $K_D^{CPX/L} = 0.23$ , consistent with the work cited above. However, the clinopyroxenes of the three samples with highest FeO\*/MgO have an apparent  $K_D^{CPX/L}$  less than 0.23. It is not certain whether this is a real feature or not. A similar plot for the Samail ophiolite (Pallister and Hopson, 1981) also shows a tendency for some clinopyroxenes with high FeO\*/MgO to have below average  $K_D^{CPX/L}$ . Clinopyroxenes have a greater FeO\*/MgO range than olivine in any one NAM sample, and some zoning is evident. Duke (1974) suggested that  $K_D^{CPX/L}$  varies with bulk liquid composition more than  $K_D^{OL/L}$ . This might account for the wider range and zoning of FeO\*/MgO in the clinopyroxenes than olivines within samples. Also, the distribution coefficients for FeO\*/MgO may vary somewhat when olivine and clinopyroxene are accompanied by other phases (Hanson and Langmuir, 1978). The NAM sample in fig. 5 with the highest FeO\*/MgO, #777, has much more hornblende than any other sample, and this might affect the distribution coefficients. Another explanation for the discrepancy of some samples is that, due to the range of FeO\*/MgO in clinopyroxenes within samples, an accurate average has not been determined.

Additional evidence that minerals in NAM adcumulates are generally in equilibrium is the sympathetic variation between olivine Mg/Mg+Fe and plagioclase Ca/Ca+Na. The linear correlation coefficient for ten NAM samples is 0.82 and figure 4 shows the relatively minor crossing of tie lines. Pallister and Hopson (1981) report similar results for the Samail ophiolite. They did suggest that the minor crossing of tie lines between mineral compositions on a similar diagram indicate true disequilibrium, and suggest this is evidence that some limited settling



occurs. This may also be the case for some NAM samples, but some of the crossing tie lines can be explained otherwise. For example, sample 909 has plagioclase Ca<sup>#</sup> more evolved than expected from the olivine, clinopyroxene, or orthopyroxene compositions. The small amount of plagioclase appears to have formed from pore liquid (figure 6) which might have fractionated in situ. Secondly, although olivine compositions within samples are constant, plagioclase and clinopyroxene show some zoning in some samples, especially isotropic gabbros, and this combined with calculated higher pore volume suggest a "mesocumulate" origin, i.e., equilibrium with the local liquid was not as well maintained as in true "adcumulates".

I believe these observations are evidence that crystallization took place quite close to the magma chamber margins. McBirney and Noyes (1979) suggested that crystallization of Skaergaard plutonic rocks took place within a thin static boundary layer and were suspended in a viscous magma until the advancing front of complete crystallization overtook them. Pallister and Hopson (1981) also concluded that most crystallization occurred in a marginal boundary layer from whence both in situ crystallization and settling took place.

Whether crystallization took place precisely in situ at the liquid-rock interface as Campbell (1978) and Casey (1980) advocate or heterogeneously throughout a static boundary layer as supported by McBirney and Noyes (1979) and Pallister and Hopson (1981) may be impossible to determine by chemical means. Both processes are similar and controlled by thermal and chemical diffusion phenomena and I don't believe any significant differences in layering, textural, and chemical features would result. The major difference between the two processes

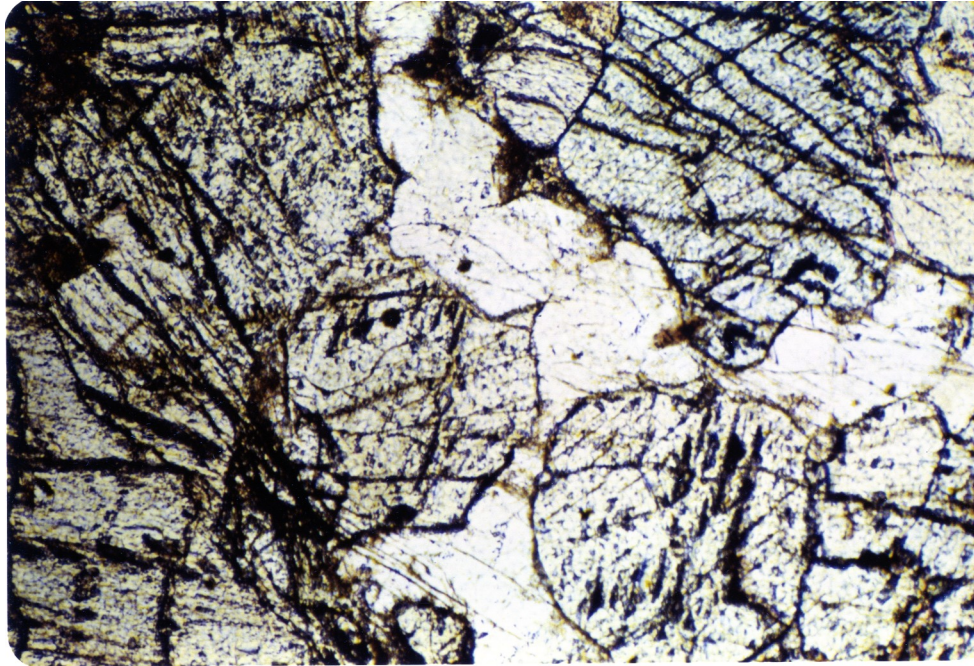


Figure 6. Sample 909A, plane light. Photomicrograph of lherzolite showing minor plagioclase interstitial to pyroxenes. This is the main occurrence of plagioclase in this rock, and its Ca# (74) indicates it crystallized from a liquid more differentiated than did the pyroxenes (Mg# = 82-84) or olivine (Fo = 81).

is simply the actual site of nucleation.

It should be possible, however, to determine if settling has taken place with detailed analytical work within and between layers. McBirney and Noyes (1979) did this with detailed mineral analyses along a traverse through a single 10cm graded layer in the Skaergaard. They found regular variations in major and minor elements in the minerals along the traverse, a feature they believed unlikely if crystal settling occurred, but which is consistent with diffusion controlled in situ crystallization. Insufficient data were collected for this study to make similar judgments.

#### 4.4 EVIDENCE OF CHEMICAL ZONATION AND MAGMA MIXING WITHIN A STEADY STATE MAGMA CHAMBER

##### 4.4.1 Whole rock chemical variation in NAM plutonic rocks

As discussed in chapter 2, whole rock compositions of plutonic rocks are difficult to interpret. However, if caution is used, some inferences can be made from the NAM whole rock data.

Irvine and Findlay (1972) noted an irregular but general increase in whole rock  $FeO^*/MgO$  with increasing stratigraphic height in the plutonic rocks of the NAM and TM massifs. They also observed similar behavior in forsterite content of olivines in the TM rocks. From these observations they concluded that the degree of fractionation of the liquid from which these rocks crystallized increased upward. They attributed the very erratic behavior to variations in the amount of trapped liquid.

Similar results were obtained in this study. Whole rock  $\text{FeO}^*/\text{MgO}$  and Zr are plotted against approximate distance upward from the harzburgite-magmatic plutonic complex boundary in figure 7. Both show a general but erratic increase upward. These trends are consistent with an upward increase in degree of fractionation of the liquid or with an upward increase in the amount of trapped pore liquid, or both. Cryptic chemical variation (section 4.4.2) and estimated amounts of trapped pore liquid (section 4.2) suggest both occur in these NAM rocks.

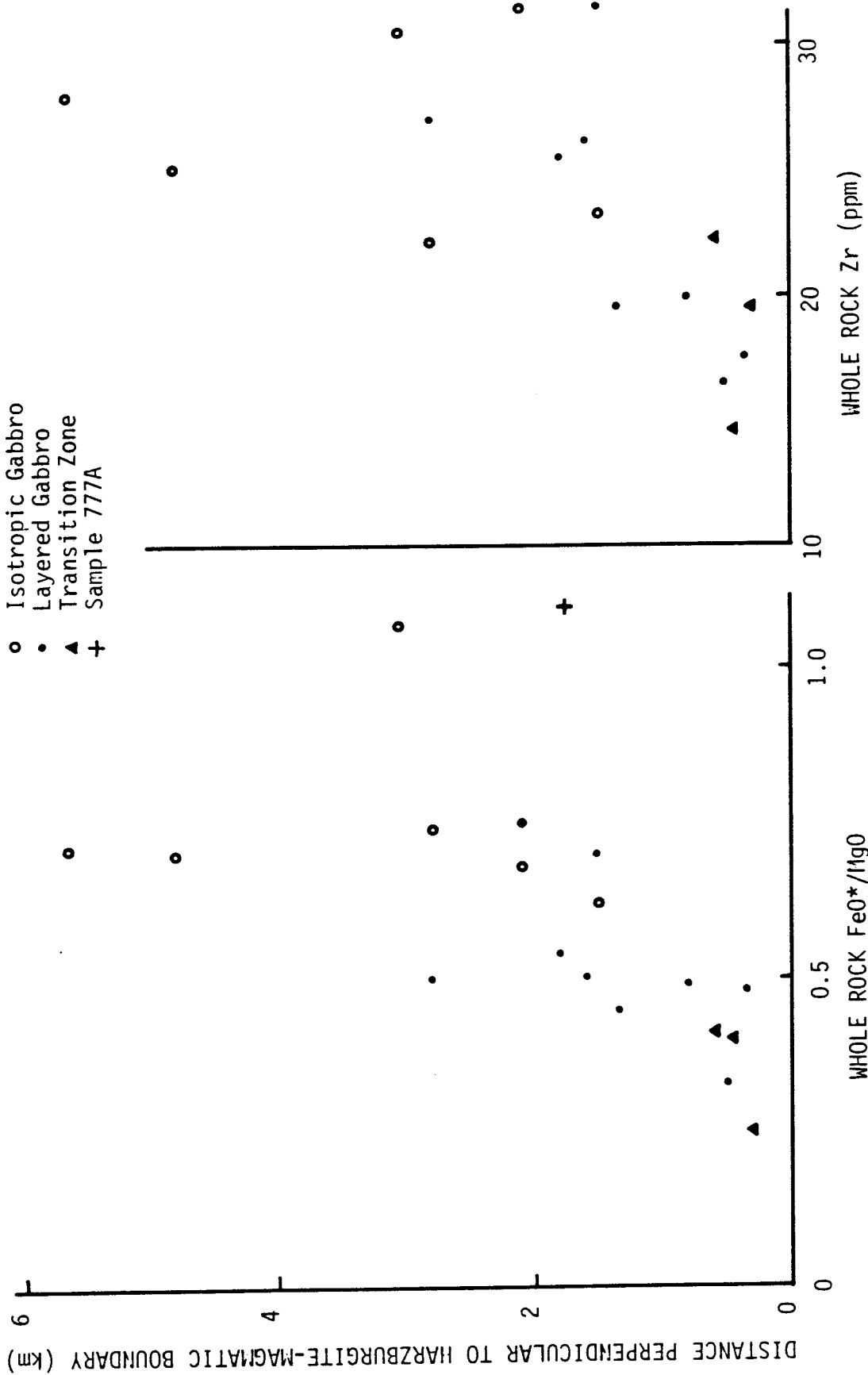
It is important to note that any single traverse upward through the plutonic section is not isochronal if indeed igneous layering outlines the shape of the former magma chamber (Casey, 1980). Therefore, vertical chemical variations may be due in part to variation in magma chemistry with time. Sampling over a wider geographic area (i.e., lateral traverses parallel to the spreading direction) is necessary to determine the extent of temporal variation.

To determine whether whole rock  $\text{FeO}^*/\text{MgO}$  is a reliable indicator of  $\text{FeO}^*/\text{MgO}$  of the liquid, whole rock  $\text{FeO}^*/\text{MgO}$  is plotted against olivine  $\text{FeO}^*/\text{MgO}$  for samples from the transition zone and layered and isotropic gabbro units (figure 8). The least squares regression fit has a correlation coefficient of 0.997. Although the scatter precludes conclusions about the relative degree of fractionation among a few samples, it appears whole rock  $\text{FeO}^*/\text{MgO}$  may indicate general fractionation trends among a large number of samples.

Figure 7. Variation in whole-rock  $\text{FeO}^*/\text{MgO}$  and Zr with height in the North Arm Mountain plutonic complex, measured perpendicular to the residual mantle-magmatic complex boundary.

KEY

- Isotropic Gabbro
- Layered Gabbro
- ▲ Transition Zone
- + Sample 777A



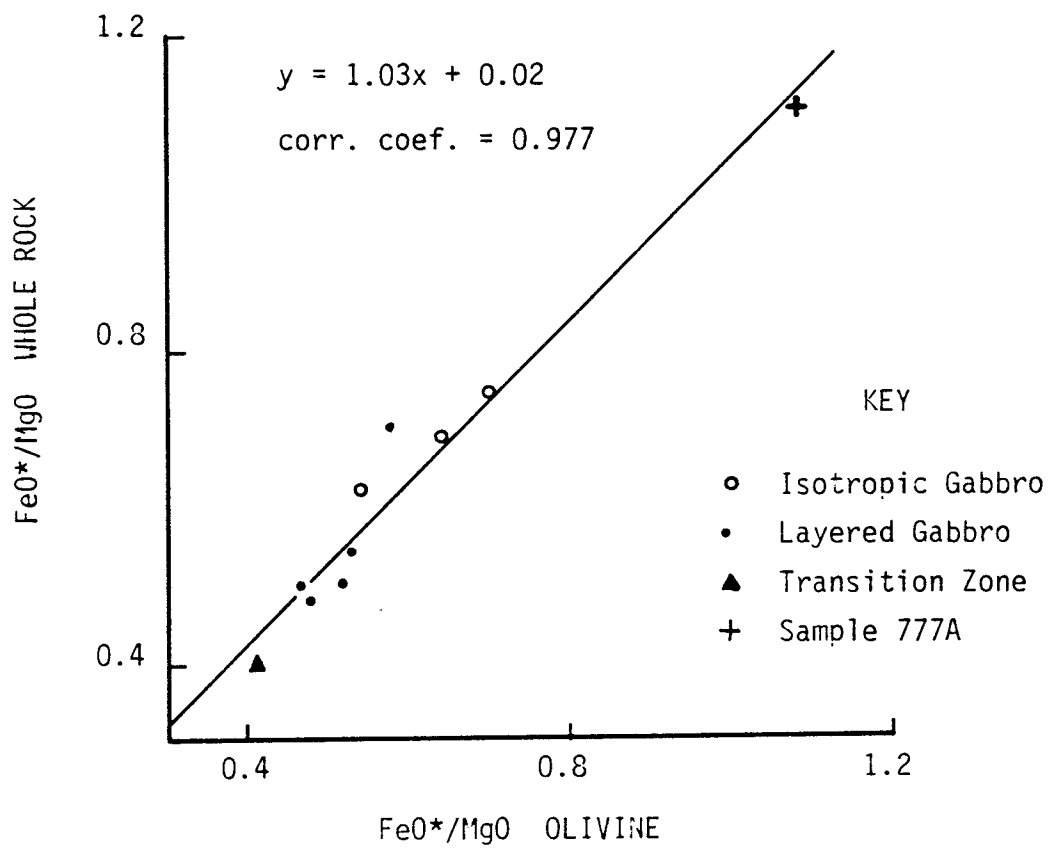


Figure 8. Correlation between whole-rock and olivine  $\text{FeO}^*/\text{MgO}$  of adcumulus-mesocumulus textured plutonic rocks. The line is a least-squares fit.

However, caution must be used with this kind of whole rock data. All of the samples in figure 8 have similar textures (adcumulate or mesocumulate) and mineralogy. The probable reason for the good correlation in figure 8 is that most of the iron and magnesium in these samples are contained in minerals with similar distribution coefficients. Therefore, the whole rock bulk distribution coefficients for  $\text{FeO}^*/\text{MgO}$  are close to that of olivine. Samples with significant amounts of minerals having  $\text{FeO}^*/\text{MgO}$  distribution coefficients significantly different than olivine, pyroxene, or hornblende (e.g., magnetite) may not be compared with these samples because whole rock  $\text{FeO}^*/\text{MgO}$  may be much different than the equilibrium local liquid.

Secondly, as Irvine and Findlay (1972) pointed out, whole rock  $\text{FeO}^*/\text{MgO}$  may be affected by the amount of trapped liquid. This seems not to be a significant factor among the adcumulates and mesocumulates in figure 8. However, orthocumulates have a larger and probably more variable amount of trapped pore liquid and therefore whole rock  $\text{FeO}^*/\text{MgO}$  should deviate more from the liquid  $\text{FeO}^*/\text{MgO}$ . Mineral chemistry was not determined for any NAM orthocumulate so the relationship between liquid and whole rock  $\text{FeO}^*/\text{MgO}$  could not be ascertained. Orthocumulates probably would not be directly comparable to adcumulates.

Although the variation in whole rock Zr doesn't distinguish between fractionation or percent trapped liquid, it is consistent with both. Inspection of estimated pore data shows a general increase upward. The good correlation between olivine and whole rock  $\text{FeO}^*/\text{MgO}$  suggests that the upward increase in  $\text{FeO}^*/\text{MgO}$  and probably Zr are at least partly due to fractionation.



#### 4.4.2 Cryptic Chemical Variation - Evidence for Magma Mixing and Chemical Zonation

Cyclic cryptic chemical variation has been considered evidence of periodic magma replenishment in some continental stratiform intrusions (e.g., Irvine, 1970) and ophiolites (e.g., Irvine and Findlay, 1972; Church and Riccio, 1977; Stern, 1979; Pallister and Hopson, 1981; Smewing, 1981). An important corollary is the relatively limited compositional range of the magma. Although sample density in this study is not suited to examine fine scale cryptic variations, enough data were obtained to demonstrate that the compositional range of the NAM magma was rather limited over a significant vertical thickness and also that the degree of fractionation of the magma increased slightly with stratigraphic height.

Various mineral chemical characteristics were determined for samples distributed over an area of 8 or 9 square kilometers (fig. 1). Seven samples lie along a SE-NW traverse which extends upward through the transition zone and layered gabbro unit. This traverse is nearly coincident with the lower part of the NAM traverse reported in Irvine and Findlay (1972). A second traverse, about 1.5 km northeast of the first, consists of one layered and three isotropic olivine gabbros displaced up to one third kilometer on either side of the traverse. Both traverses are crudely perpendicular to major lithologic contacts and fine scale igneous layering. Fine scale igneous layering becomes somewhat oblique near the upper part of the traverses, but not as much as in other areas of NAM.

The range in mineral compositions of most samples in this area is quite limited. The total range in Fo content of olivines of 9 samples

is 72-81. The range in  $\text{Ca}^\#$  of plagioclases of 10 samples is 61-78. Sample 777 has  $\text{Fo}_{62}$  and  $\text{Ca}^\#_{60}$  and in every respect is anomalously highly fractionated relative to other rocks in the layered units. It has abundant primary brown hornblende and incompatible trace element concentrations close to diabase 109. The most plausible origin of this sample is that it crystallized from a body of segregated pore liquid, or more in accord with its adcumulus texture, from fractionated liquid migrating through a conduit, similar to veins and dikes observed by Casey (1980) cutting the lower ultramafic and transition zone rocks.

Irvine and Findlay (1972) found a range of  $\text{Fo}_{77-86}$  in olivines of four Table Mountain olivine gabbros, and  $\text{Fo}_{84-91}$  in Table Mountain dunitic olivines. Unfortunately they determined olivine  $\text{Fo}$  of only one sample from their NAM traverse.

Olivine  $\text{Fo}$  and plagioclase  $\text{Ca}^\#$  of samples along the two traverses of this study are plotted against relative distance perpendicular to the harzburgite-magmatic boundary in figure 9. Lithologic unit boundaries are also shown and in effect superimpose the cryptic variation trends on a map view of the area. The limited range is evident and especially notable in the southwestern traverse in view of the diverse nature of rock types in this traverse (a lherzolite, troctolite, and four olivine gabbros). The greater variation in  $\text{Ca}^\#$  of plagioclase is probably due to mild zoning, especially in isotropic gabbros, and greater variability in  $K_D$ 's of plagioclase components.

There is a slight decrease in  $\text{Fo}$  and  $\text{Ca}^\#$  upward, especially in the isotropic gabbros of the northeastern traverse. This is consistent with the hypothesis that there is a general increase in the degree of fractionation upward, especially between major lithologic units, as

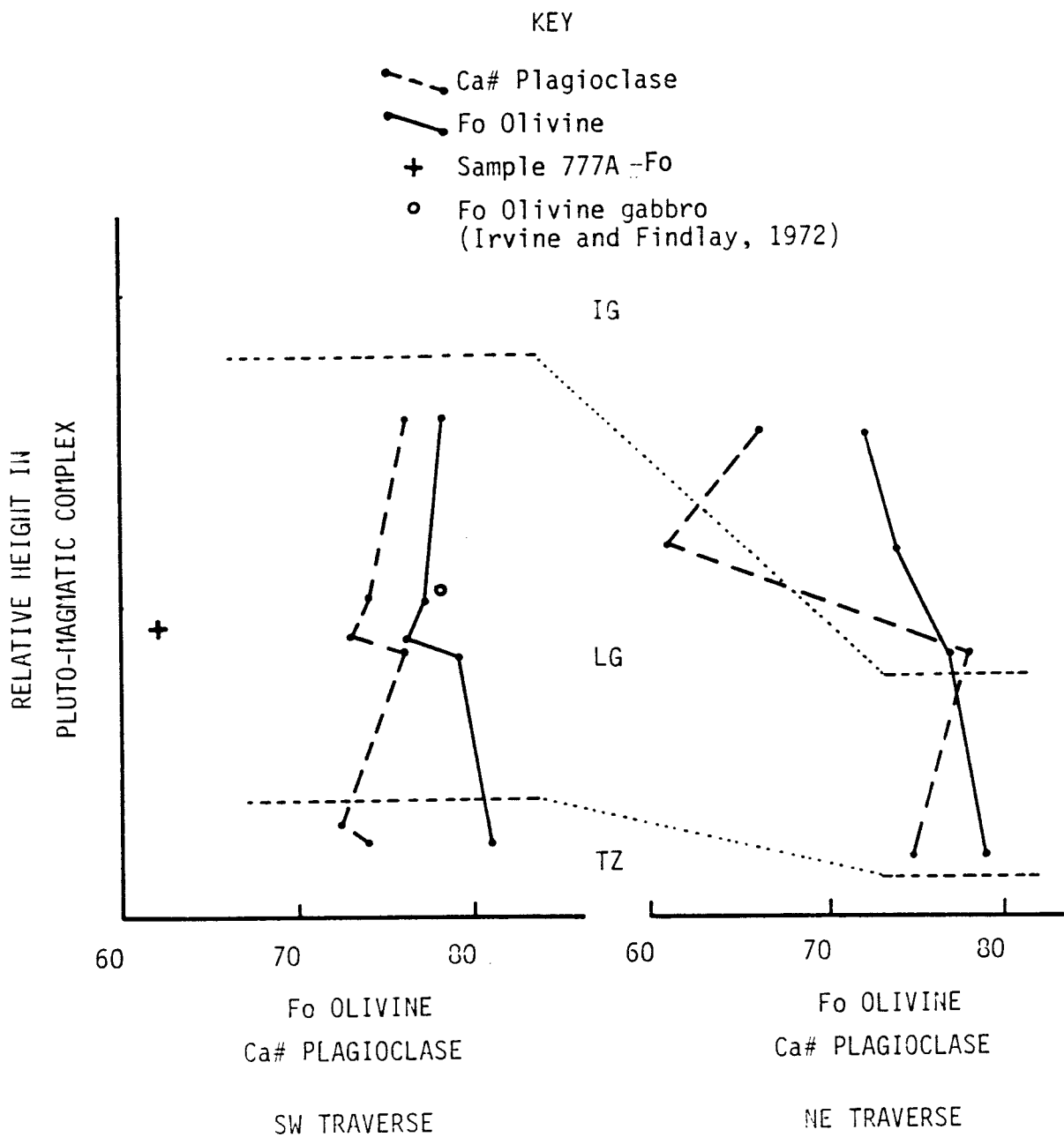


Figure 9. Cryptic variation in olivine Fo and plagioclase Ca# with relative height in the transition zone and gabbroic units of North Arm Mountain. Samples are those represented with open circles in figure 1.

suggested by Irvine and Findlay (1972) and Church and Riccio (1977) and consistent with whole rock chemical variation discussed in section 4.4.1.

These observations are similar to those made in the Oman ophiolite (Pallister and Hopson, 1981; Smewing, 1981) but unlike the Oman, cryptic reversals on NAM are not accompanied by changes to more mafic mineral assemblages. This may imply the magma of NAM was more efficiently buffered, at least in the area of these samples. Variations in whole rock Mg/Mg+Fe along a NAM and a Table Mountain traverse (Irvine and Findlay, 1972) indicate the liquid from which the TM olivine gabbros crystallized may have been more variable and more highly fractionated near the top than the NAM magma. Too little mineral chemistry is available to confirm this. If the constancy of chemistry and mineralogy of gabbros in this area of NAM are due to more efficient buffering, a more steady supply of fresh magma concomitant with an increase in spreading rate in this area may be the possible cause.

The cryptic chemical evidence presented here and by Irvine and Findlay (1972) and Church and Riccio (1977) suggest the presence of a steady state magma chamber and thus magma mixing were important features responsible for producing the Bay of Islands ophiolite. Similar evidence is reported for several other ophiolites.

## CHAPTER 5

### NAM MINERAL ASSEMBLAGES

#### 5.1 INTRODUCTION

A wide variety of mineral assemblages which cannot be produced solely by simple crystal fractionation of a single liquid are observed in the plutonic rocks of ophiolites. Furthermore, it is likely, based on geologic evidence, that multiple magma chambers were not present, at least in the Bay of Islands (Casey, 1980), but that most or all of the plutonic rocks formed from a single large open system chamber. Mixing of magmas combined with crystal fractionation in such a system can produce much of the variability, but not all of it. This chapter explores some of the processes which may be responsible for some of the variation in mineral assemblages.

#### 5.2 CRYSTALLIZATION SEQUENCE OF THE NAM PARENT MAGMA

Church and Riccio (1977) classified ophiolites on the basis of inferred crystallization sequences. They observed that many ophiolite "cumulate" sections apparently exhibit more than one order which cannot be related by crystal fractionation, and that these sequences vary among ophiolites. They attributed the variability in crystallization order to such phenomena as variable parent compositions due possibly to different degrees of partial melting and to variability in the mantle source, and to the open system nature of the magma chambers.

Church and Riccio (1977) concluded that there were two main crystallization orders in the Bay of Islands plutonic rocks, the ultramafic rocks following the order ol-pl-cpx-opx, and the mafic rocks following the order ol-pl-cpx-opx. They based this

conclusion mainly on rock textures. Malpas (1978) also concluded the minerals in the gabbros crystallized in the sequence ol-pl-cpx-opx, based on rock textures and the fact that many lavas and dike rocks plotted near the natural basalt system plagioclase-diopside cotectic in the normative basalt tetrahedron.

Whether or not these crystallization orders are correctly interpreted is debatable. Some workers (e.g., Campbell, 1978; McBirney and Noyes, 1979, Casey, 1980) believe the rock textures which are normally interpreted to indicate crystallization order (e.g., inclusive relationships) are equally compatible with simultaneous crystallization controlled by nucleation energies and diffusion rates. Therefore, considering the preponderance of three-phase gabbros and their adcumulus texture, it seems likely that these crystallized by co-precipitation of all three phases near the liquidus temperature (Casey, 1980). The presence of minor orthopyroxene without plagioclase in the ultramafic and transition zone rocks is as yet unexplained.

In any event, it is necessary to distinguish between crystallization order of a particular rock or rock group and the low pressure crystallization order of the parent magma. In an open system, magma mixing can produce hybrid liquids having crystallization orders different from the parent.

The overall crystallization order of the NAM parent magma was probably ol ( $\pm$ chr)-cpx-pl-opx. The general order of appearance of volumetrically significant primocryst minerals, from base to the top of the plutonic complex, is olivine, clinopyroxene, and finally plagioclase, with some opx replacing olivine in the uppermost gabbros. Other minerals (i.e., hornblende, Fe-Ti oxides) are volumetrically insignifi-

cant and therefore are not included in the main crystal sequence.

Furthermore, mineral chemistry is consistent with this sequence. Olivine is the most primitive mineral found in significant amounts, with basal dunites having olivine with  $Fo_{90-91}$  (Irvine and Findlay, 1972; Church and Riccio, 1977; Malpas, 1978). Olivine is also fairly ubiquitous in all but the upper isotropic gabbro. Therefore, it follows that most of the plutonic rocks formed from olivine saturated liquids.

Dunite becomes interlayered with clinopyroxene bearing rocks upward, with forsterite content dropping into the upper eighties (Church and Riccio, 1977). Clinopyroxene is nearly ubiquitous in all but the lower dunites, and it seems likely that it was the second major phase to crystallize.

Plagioclase is found in very minor amounts in the ultramafic rocks, but becomes increasingly abundant through the transition zone until it is the dominant phase in the gabbros. The most primitive plagioclase found in this study was  $Ca^{\#} = 79$  in the lower gabbro. Church and Riccio (1977) report plagioclase with  $An_{84}$  (at these low  $K_2O$  contents,  $An$   $Ca^{\#}$ ) in a lower gabbro of North Arm Mountain. The  $Fo$  and  $Mg^{\#}$  of olivines and clinopyroxenes has dropped to the lower eighties at this level. It seems likely, then, that plagioclase was the third phase to crystallize.

This crystallization sequence results in the majority of NAM plutonic rocks being dunite, wehrlite, and olivine gabbro, with lesser amounts of intermediate members of this suite (e.g., olivine clinopyroxenites, feldspathic wehrlites, etc.). Minor variants include almost every combination of olivine, clinopyroxene, plagioclase, and orthopyroxene.

### 5.3 MAGMA CHAMBER PROCESSES INFERRED FROM NORTH ARM MOUNTAIN MINERAL ASSEMBLAGES

#### 5.3.1 Main Sequence Assemblages

If the mineral assemblages of NAM are primary equilibrium assemblages (see section 4.3), the main crystallization sequence can easily be attributed to simple equilibrium crystal fractionation, the extent of which is limited by mixing of newly injected primitive magma. This is diagrammatically shown in the simplified basalt tetrahedron (figure 10), where the parent magma N, located in the olivine phase volume, fractionates to the olivine-clinopyroxene cotectic by crystallization of olivine, thus producing the basal dunites. The wehrlitic lithologies of the upper ultramafic zone are produced by co-precipitation of olivine and clinopyroxene, which drives the liquid to the olivine + clinopyroxene + plagioclase cotectic, where crystallization of olivine gabbro moves the liquid toward the quaternary pseudo-invariant point, p. The four-phase pseudo-invariant point is seldom reached in the lower NAM plutonic rocks, except possibly by fractionating trapped pore liquid. Only in the upper orthocumulus gabbros is there evidence that any liquid ever fractionates beyond this point.

This is nearly the same scenario as described by Pallister and Hopson (1981) for the south Oman, except that they believe the parent magma of that ophiolite fractionated directly to the 3-phase cotectic because plagioclase and clinopyroxene appear simultaneously in the layered sequence.

Maintenance of this sequence and the limiting of further fractionation is due to repeated mixing of new batches of parental magma.



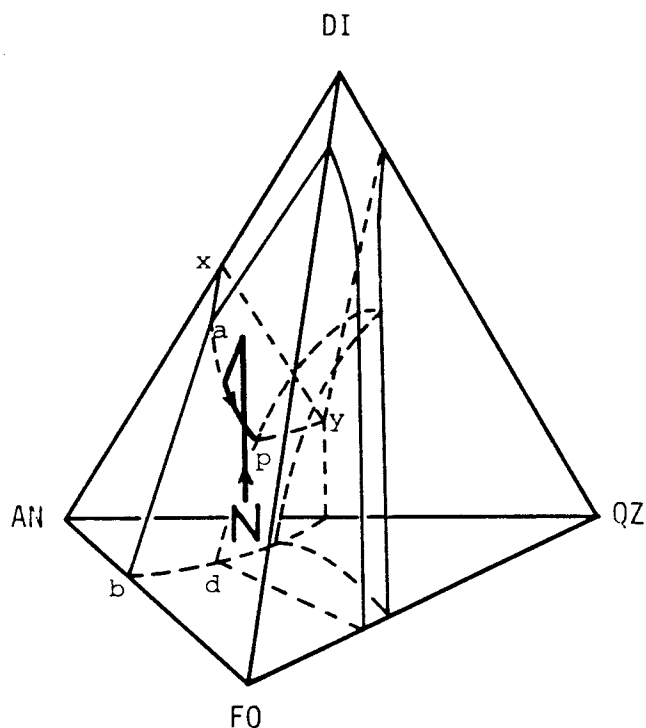


Figure 10. Diagrammatic representation of the overall crystallization sequence of the NAM parent magma (N). Crystallization of liquidus forsteritic olivine drives the liquid to 2-phase (ol+cpx) saturation, from which point co-precipitation drives the liquid to ol+cpx+plag saturation. Mixing of fractionated liquids on or near the 2 or 3-phase cotectics may produce olivine undersaturated hybrids from which non-olivine bearing gabbros crystallize. Normative basalt tetrahedron modified (for clarity) from Presnall, et. al. (1978).

Furthermore, the composition of the NAM parent magma must have been relatively constant with time, at least in respect to its projection toward the clinopyroxene phase volume, as evidenced by the very small amounts of variant assemblages such as troctolites or orthopyroxenites or websterites. This appears not to be the case in north Oman (Smewing, 1981), where orthopyroxene replaces clinopyroxene as the second primary phase in some places.

It is important to note that mixing of the parent magma with any liquid along the main fractionation path can only result in hybrid liquids in the olivine phase volume. Fractionation of these hybrids will return them to the olivine + clinopyroxene or 3-phase cotectics. The only exception to this is if the parent is mixed with a liquid which has fractionated past the quaternary pseudo-invariant point (i.e., is cpx-opx-pl saturated), a possibility discussed in the next section.

### 5.3.2 Variant Mineral Assemblages

There are many variant mineral assemblages in the NAM plutonic rocks which cannot be produced from a single parent composition by the process outlined in the preceding section. These variants include troctolites and anorthosites, rare primary orthopyroxene bearing rocks, and non-olivine gabbro. Except for the gabbro, these variants are volumetrically minor. Some of the possible processes responsible for these variants are discussed in this section.

### 5.3.2.1 Variability in parent magma composition

As already discussed, fractionation of the NAM parent by olivine crystallization generally moves the liquid toward the clinopyroxene phase volume. If the composition of the parent were variable enough, it could fractionate to any of the two-phase or three-phase cotectics involving olivine. This could result in either plagioclase or orthopyroxene following olivine in the crystallization sequence, and the troctolites and orthopyroxene bearing rocks may be produced. Smewing (1981) suggested parent variability, possibly due to partial melting or pre-fractionation variations, may be responsible for the occurrence of two main crystallization sequences in north Oman, one in which clinopyroxene follows olivine and one in which orthopyroxene follows olivine. He cited the wide range in mineral compositions and assemblages of dikes cutting the harzburgite as additional evidence of parent variability.

Although troctolites and orthopyroxene bearing variants (e.g., the lherzolite sample 909A in this study) occur on NAM, they are volumetrically minor and isolated, and it seems unlikely that they may be due to parent variability. It seems the NAM parent, like that of the south Oman (Pallister and Hopson, 1981) was less variable than that of the north Oman, at least with respect to its projection toward the clinopyroxene phase volume.

However, olivine gabbro is conformable with residual harzburgite for a distance along strike of the major lithologic contacts of about 4 km on North Arm Mountain. This may indicate that either a temporary decrease or cessation of magma influx occurred whereby fractionation proceeded further or where mixing of the parent was more efficient, or

that the parent was three-phase saturated. The general thinning of the crust in this area supports the former hypothesis, I suggest.

#### 5.3.2.2. Mixing of evolved liquids

A second type of mixing, unlike that previously discussed (mixing of newly introduced parent magma), involves mixing of liquids already fractionated from the parent composition. Irvine (1979) has shown that mixing liquids of appropriate compositions can produce virtually any crystallization order among olivine, clinopyroxene, plagioclase, and orthopyroxene in the basalt system.

However, this process cannot be used to explain all of the observed variants because of limitations in the possible liquids available for mixing. For example, as Irvine demonstrated, mixing of a NAM main sequence liquid with a liquid which had fractionated beyond the quaternary pseudo-invariant point can produce hybrids capable of crystallizing orthopyroxene before plagioclase or clinopyroxene. This may explain the occasional primary orthopyroxene bearing rocks found in the ultramafic and transition zones. However, I don't believe this to be the case. This process would require a source of liquid which had fractionated beyond the 4-phase pseudo-invariant point, and the only likely source is the liquid from which the uppermost orthocumulus gabbros crystallized. This seems unlikely because of the spatial separation of the two rock types. However, it may be possible that a hybrid liquid formed in this way near the top of the chamber could be transported to the lower regions by convection without significant further crystallization. Due to the pressure dependence of the liquidus temperature of a liquid, eventually

this liquid will crystallize in the lower portions of the chamber (Jackson, 1961; Irvine, 1970).

Mixing of two fractionated liquids which both lie on the ol-cpx-pl cotectic has been proposed by Walker, et al., (1979) as a way to produce hybrid liquids capable of advancing clinopyroxene before olivine in the crystallization sequence. This is due to the compositional curvature of the 3-phase cotectic. Pallister and Hopson (1981) suggested this mechanism might have been responsible for producing the non-olivine gabbros of south Oman. Whether such hybrid liquids lie in the clinopyroxene or plagioclase phase volumes or on the cpx-pl cotectic surface depends on the sense of curvature of the cpx-pl surface (plane a-p-y-x in figure 10). This curvature is unknown except in the 3-component (Di-An-SiO<sub>2</sub>) system.

If such a mixing process is assumed to be the cause of non-olivine gabbro, field evidence may shed some light on the sense of curvature of the cpx-pl cotectic surface and perhaps place some constraints on this mixing process.

The vast majority of rocks in the gabbroic units of NAM are gabbro and olivine gabbro. These two lithologies are randomly distributed laterally, but there is a general decrease in the olivine gabbro upward in the isotropic gabbros. Either type may be aurally extensive or intimately interlayered with each other. Minor troctolite persists throughout the layered section, and anorthosite and feldspathic dunites and clinopyroxenites are scattered throughout the lower layered gabbros. Mineral proportions vary within and between layers.

If the cpx-pl cotectic is markedly curved, and mixing along the 3-phase cotectic occurs, either clinopyroxenites or anorthosites should

results. Both of these variants are observed, but in minor amounts. The lack of extensive amounts of either suggests 1) the cpx-pl cotectic surface is only slightly if at all curved near the 3-phase cotectic, or 2) mixing produces hybrids only slightly removed from the 3-phase cotectic, so that precipitation of the liquidus phase results in rapid return to 2 or 3-phase saturation, perhaps within the same rock that the liquidus phase first begins to crystallize, or 3) other processes are responsible for producing the observed mineral assemblages.

In any event, mixing of this type should produce hybrids which crystallize olivine after clinopyroxene and plagioclase due to the curvature of the olivine-clinopyroxene-plagioclase cotectic into the olivine field relative to the plagioclase and clinopyroxene field in the CMAS projections of Walker, et. al., (1979) (see also Stolper, 1980, for the projection from cpx). The presence of minor troctolites and wehrlites suggests that either the mixing process is more complex, with mixing of several orders of hybrids, or that other processes are responsible for these rocks.

#### 5.3.2.3 Disequilibrium crystal fractionation and diffusion and discontinuous nucleation effects on mineral assemblages

Previous discussion has assumed that equilibrium crystallization has occurred, that is, crystallization of pertinent phases occurred when saturation was reached. This is probably not strictly true because a certain amount of supersaturation (nucleation activation energy) is usually necessary to initiate nucleation. McBirney and Noyes (1979) have proposed a model by which fine scale igneous layer-

ing may be produced by discontinuous nucleation controlled by thermal and chemical diffusion rates. Basically, this model proposes that once a phase nucleates, crystallization will tend to deplete the local liquid in the components of that phase. As crystallization proceeds, eventually the zone of depletion will not be able to be replenished fast enough by chemical diffusion, and crystallization of that phase will decrease or cease. Renewed nucleation will occur when favorable thermal and chemical conditions are restored.

In a multi-component system, depletion of components of one phase enhances the concentrations of other components, and continued growth of the already nucleated phase may cause supersaturation of other components. Nucleation of a new phase will result when the nucleation activation energy is reached.

As an example, crystallization of olivine, which nucleates easily, may drive the liquid toward the ol-cpx or ol-pl cotectic surface. Owing to the nucleation activation energy of these phases, the trend of the liquid may "pierce" the cotectic surface, resulting in a hybrid within the clinopyroxene or plagioclase phase volumes.

McBirney and Noyes' (1979) calculations based on reasonable diffusion rates restrict this process to a relatively fine scale, probably no more than one meter. Nevertheless, it can explain some of the minor variant assemblages observed in ophiolite plutonic rocks.

#### 5.4 CONCLUSIONS

It seems that no single process is capable of producing the wide variety of mineral assemblages observed in ophiolites. I have briefly discussed a few of these processes and their limitations in explaining

mineral assemblage variations. As Casey (1980) observed, many complex processes must operate within these ocean floor magma chambers. Detailed mineralogical and chemical study is necessary to solve the puzzle.



## CHAPTER VI

### SUMMARY AND SUGGESTIONS FOR STUDY

The mineralogic and chemical features discussed in this thesis and the geologic and structural observations made by Casey (1980) and other workers suggest the following:

1. The NAM massif of the Bay of Islands ophiolite probably formed at a mid-ocean spreading center.
2. The magma from which the volcanics and dikes formed was tholeiitic.
3. Forsteritic olivine ( $\text{Fo}_{90-91}$ ) was the liquidus phase of the parent magma. The overall crystallization sequence of this magma was probably ol-cpx-pl-opx.
4. The magma from which the plutonic rocks crystallized was zoned, with the degree of fractionation increasing upward.
5. Magma mixing was a prominent process, and repeated influx of parent liquid limited the extent of differentiation.
6. Textural, chemical, and structural evidence are more consistent with in situ crystallization than crystal settling as the dominant plutonic rock-forming mechanism.
7. No single process can account for the mineralogic complexity of the plutonic rocks.

The North Arm Mountain massif provides a well preserved cross-section of old ocean crust. This massif preserves two prominent features which are lacking or not yet well defined in most other ophiolites. The first is the well constrained outline of the magma chamber, assuming Casey's (1980) interpretation regarding igneous layering is correct.

The second is the continuous lateral variation in lithology and structure parallel to the presumed spreading direction (figure 1). This massif, then, provides perhaps a unique opportunity to study the processes responsible for variations in ocean crust and magma chamber rheology.

I believe that the most likely explanation of this lateral variation in the NAM massif is like that alluded to by Casey (1980, figure 7UU, p. 483) in that the size and shape of the magma chamber changed with time, perhaps concomitant with a change in spreading rate. Where the layered gabbro is conformable with residual harzburgite in the northeastern part of Casey's map area, the plutonic complex thins, and the angle between igneous layering and the magmatic-residual contact increases. This is suggestive that the size of the chamber temporarily decreased in this area. This and the pinching out of the magmatic ultramafic and transition zone rocks is consistent with the interpretation that the supply of parent magma temporarily decreased or ceased. Also, the ratio between the thickness of isotropic to layered gabbro increases in this area. This may have resulted from a rapid rate of heat loss extending deeper into the crust, thus preventing development of igneous layering by the double diffusive mechanism of McBirney and Noyes (1979). Such a process might be expected if thermal input via magma influx decreased or ceased. Other processes (e.g., rapid cooling due to increased hydrothermal circulation) can, however, also explain the increased thickness of non-layered gabbros (Casey, personal communication, 1981).

In any event, the opportunity exists to determine what, if any, chemical variations may be related to the change in these magma chamber and crustal characteristics with time. In view of these and other

considerations discussed in this thesis, I recommend that:

1. Detailed mineral chemical data should be obtained from lateral traverses (parallel to the spreading direction) across both the thin and thick areas of the plutonic rocks, for the purpose of determining the presence and character of associated magma compositional variations in the hope of elucidating the processes contributing to such variability.
2. Detailed mineral chemical data (including minor elements) should be collected within and between fine scale igneous layers for the purpose of determining if in situ diffusion controlled fractionation contributed to the formation of this layering (i.e., in a manner similar to the work of McBirney and Noyes, 1979).
3. Additional whole rock major and trace element compositions of extrusive and hypabyssal rocks be obtained to provide a better data base for modelling chemical variations, for example in rock formation mechanisms. Furthermore, high quality analyses of incompatible trace elements at lower detection limits than obtained in this study are needed for this type modelling.

First order processes contributing to crustal accretion at divergent plate boundaries are becoming fairly well known. It is hoped that studies like those suggested above will lead to a better understanding of more detailed processes operating in mid-ocean ridge magma chambers.

## REFERENCES CITED

- Campbell, I.H., 1978. Some problems with the cumulus theory, Lithos, 11, 311-321.
- Casey, J.F., 1980. Geology of the southern part of the North Arm Mountain massif, Bay of Islands Ophiolite Complex, western Newfoundland, with application to ophiolite obduction and the genesis of the plutonic portions of oceanic crust and upper mantle.  
Unpub. Ph.D. dissertation, State University of New York at Albany.
- Casey, J.F., J.F. Dewey, P.J. Fox, J.A. Karson, and E. Rosencrantz, 1979. Heterogeneous nature of oceanic crust and upper mantle: A perspective from the Bay of Islands Ophiolite, in The Sea, vol. III, Emiliani, C., ed., New York, John Wiley.
- Casey, J.F., and W.S.F. Kidd, 1981. A parallochthonous group of sedimentary rocks unconformably overlying the Bay of Islands ophiolite complex, North Arm Mountain, Newfoundland, Can. J. Earth Sci., 18, 1035-1050.
- Church, W.R. and R.A. Coish, 1976. Oceanic versus island arc origin of ophiolites, Earth Planet. Sci. Lett., 31, 8-41.
- Church, W.R. and L. Riccio, 1977. Fractionation trends in the Bay of Islands Ophiolite of Newfoundland: polycyclic cumulate sequences in ophiolites and their classification, Can. J. Earth Sci., 14, 1156-1165.
- DeLong, S.E. and P. Lyman, (in press). Water Capture in rapid silicate analysis.
- Dewey, J.F. and W.S.F. Kidd, 1977. Geometry of plate accretion, Geol. Soc. Amer. Bull., 88, 960-968.

- Drake, M.J., 1976. Plagioclase-melt equilibria, Geochim. Cosmochim. Acta, 40, 457-465.
- Duke, J.M., 1976. Distribution of the period four transition elements among olivine, calcic clinopyroxene, and mafic silicate liquid: experimental results, J. Petrol., 17, 499-521.
- Elthon, D., 1979. High magnesia liquids as the parental magma for ocean floor basalts, Nature, 278, 514-518.
- Hanson, G.N. and C.H. Langmuir, 1978. Modelling of major elements in mantle-melt systems using trace element approaches, Geochim. Cosmochim. Acta, 42, 725-741.
- Hart, S.R., A.J. Erlank, and E.J.D. Kable, 1974. Sea floor alteration: some chemical and Sr isotopic effects, Contr. Mineral. Petrol., 44, 219-230.
- Irvine, T.N., 1979. Rocks whose composition is determined by crystal accumulation and sorting, in The Evolution of the Igneous Rocks, H.S. Voder, ed., 245-306.
- Irvine, T.N. and T.C. Findlay, 1972. Alpine type peridotite with particular reference to the Bay of Islands igneous complex, Pub. Earth Phys. Br. Dept. Energy, Mines, and Resources, Can., 42, 97-128.
- Jackson, E.D., H.W. Green, and E.M. Moores, 1975. The Vourinos Ophiolite, Greece: cyclic units of lineated cumulates overlying harzburgite tectonite, Geol. Soc. Am. Bull., 86, 390-398.
- Jacobson, S.B. and G.J. Wasserburg, 1979. Nd and Sr isotopic study of the Bay of Islands Ophiolite Complex and the evolution of the source of midocean ridge basalts, J. Geophys. Res., 84, 7429-7445.

- Karson, J.A., 1977. The geology of the northern Lewis Hills, western Newfoundland, Unpub. Ph.D. dissertation, State University of New York at Albany, 474p.
- Karson, J.A. and J.F. Dewey, 1978. Coastal Complex, western Newfoundland: an early Ordovician oceanic fracture zone, Geol. Soc. Am. Bull., 89, 1037-1049.
- Kushiro, I., 1960. Si-Al relation in clinopyroxenes from igneous rocks, Am. J. Sci., 258, 548-554.
- MacDonald, G.A. and T. Katsura, 1964. Chemical composition of Hawaiian Lavas, J. Petrol., 5, 82-133.
- Malpas, J., 1978. Magma generation in the upper mantle, field evidence from ophiolite suites, and application to the generation of oceanic lithosphere, Phil. Trans. R. Soc. Lond., A 288, 527-546.
- Malpas, J., 1979. The dynamothermal aureole of the Bay of Islands Ophiolite suite, Can. J. Earth Sci., 16, 2086-2101.
- McBirney, A.R. and R.M. Noyes, 1979. Crystallization and layering of the Skaergaard Intrusion, J. Petrol., 20, 487-554.
- Miyashiro, A., 1973. The Troodos ophiolite complex was probably formed in an island arc, Earth Planet. Sci. Lett., 19, 218-229.
- Miyashiro, A., 1975. Classification, characteristics, and origin of ophiolites, J. Geol., 83, 249-281.
- Nelson, K.D., and J.F. Casey, 1979. Ophiolitic detritus in the Upper Ordovician flysch of Notre Dame Bay and its bearing on the tectonic evolution of western Newfoundland, Geology, 7, 27-31.
- O'Hara, M.J., 1977. Geochemical evolution during crystallization of a periodically refilled magma chamber, Nature, 266, 503-507.

- Pallister, J.S. and C.A. Hopson, 1981. Samail Ophiolite plutonic suite: field relations, phase variation, cryptic variation and layering, and a model of a spreading ridge magma chamber, J. Geophys. Res., 86, 2593-2644.
- Pallister, J.S. and R.J. Knight, 1981. Rare-earth element geochemistry of the Samail Ophiolite near Ibra, Oman, J. Geophys. Res., 86, 2673-2697.
- Pearce, J.A. and J.R. Cann, 1973. Tectonic setting of basic volcanic rocks determined using trace element analyses, Earth Planet. Sci. Lett., 19, 290-300.
- Pearce, J.A. and M.J. Norry, 1979. Petrogenetic implications of Ti, Zr, Y, and Nb variations in volcanic rocks, Contrib. Mineral. Petrol., 69, 33-47.
- Philpotts, J.A., C.C. Schnetzler, and S.R. Hart, 1969. Submarine basalts: some K, Rb, Sr, Ba, rare-earth, H<sub>2</sub>O, and CO<sub>2</sub> data bearing on their alteration, modification by plagioclase, and possible source materials, Earth Planet. Sci. Lett., 7, 293-299.
- Presnall, D.C., S.A. Dixon, J.R. Dixon, T.H. O'Donnell, N.L. Brenner, R.L. Schrock, and D.W. Dycus, 1978. Liquidus phase relations on the join diopside-forsterite-anorthite from 1 atm to 20 kbar: their bearing on the generation and crystallization of basaltic magma, Contrib. Mineral. Petrol., 66, 203-220.
- Riccio, L., 1976. Stratigraphy and petrology of the peridotite-gabbro component of the western Newfoundland ophiolites, Unpub. Ph.D. dissertation, University of Western Ontario, London, Ontario, 265p.

- Roeder, P.L. and R.F. Emslie, 1970. Olivine-liquid equilibrium, Contr. Mineral. Petrol., 29, 275-289.
- Rosencrantz, E.J., 1979. The Geology of the Northern Part of North Arm Massif, Bay of Islands Ophiolite Complex, Newfoundland: with Application to Upper Oceanic Crust Lithology, Structure, and Genesis, Unpub. Ph.D. dissertation, State University of New York at Albany, 250p.
- Seguin, M.K. and R. Laurent, 1975. Petrologic features and magnetic properties of pillow lavas from the Thetford Mines ophiolite (Quebec), Can. J. Earth Sci., 12, 1406-1420.
- Shibata, T., S.E. DeLong, and D. Walker, 1979. Abyssal tholeiites from the Oceanographer Fracture Zone I: petrology and fractionation, Contrib. Mineral. Petrol., 70, 89-102.
- Shibata, T., G. Thompson, and F.A. Frey, 1979. Tholeiitic and alkali basalts from the Mid-Atlantic Ridge at 43° N, Contrib. Mineral. Petrol., 70, 127-141.
- Smewing, J.D., 1981. Mixing characteristics and compositional differences in mantle-derived melts beneath spreading axes: evidence from cyclically layered rocks in the ophiolite of north Oman, J. Geophys. Res., 86, 2645-2659.
- Sparkes, R.S.J., P. Meyer, and H. Sigurdsson, 1980. Density variation amongst mid-ocean ridge basalts: implications for magma mixing and the scarcity of primitive lavas, Earth Planet. Sci. Lett., 46, 419-430.
- Stern, C., 1979. Open and closed system igneous fractionation within two Chilean ophiolites and the tectonic implications, Contrib. Mineral. Petrol., 68, 243-258.



- Stolper, E., 1980. A phase diagram for mid-ocean ridge basalts: preliminary results and implications for petrogenesis, Contrib. Mineral. Petrol., 74, 13-27.
- Stolper, E. and D. Walker, 1980. Melt density and the average composition of basalt, Contrib. Mineral. Petrol., 74, 7-12.
- Sun, S. and R.W. Nesbitt, 1978. Geochemical regularities and genetic significance of ophiolitic basalts, Geology, 6, 689-695.
- Sun, C., R.J. Williams, and S. Sun, 1974. Distribution coefficients of Eu and Sr for plagioclase-liquid and clinopyroxene-liquid equilibria in oceanic ridge basalt: an experimental study, Geochim. Cosmochim. Acta, 38, 1415-1433.
- Suen, C.J., F.A. Frey, and J. Malpas, 1979. Bay of Islands ophiolite suite, Newfoundland: petrologic and geochemical characteristics with emphasis on rare earth element geochemistry, Earth Planet. Sci. Lett., 45, 337-348.
- Vallance, T.G., 1974. Spilitic degradation of tholeiitic basalt, J. Petrol., 15, 79-96.
- Wager, L.R., G.M. Brown, and W.J. Wadsworth, 1960. Types of igneous cumulates, J. Petrol., 1, 73-85.
- Walker, D., T. Shibata, and S.E. DeLong, 1979. Abyssal tholeiites from the Oceanographer Fracture Zone II: phase equilibria and mixing, Contrib. Mineral. Petrol., 70, 111-125.
- Williams, H., 1975. Structural succession, nomenclature, and interpretation of transported rocks in western Newfoundland, Can. J. Earth Sci., 12, 1874-1894.

Williams, H. and J.G. Malpas, 1972. Sheeted dikes and brecciated dike rocks within transported igneous complexes, Bay of Islands, western Newfoundland, Can. J. Earth Sci., 9, 1216-1229.

Winchester, J.A. and P.A. Floyd, 1976. Geochemical magma type discrimination: application to altered and metamorphosed basic igneous rocks, Earth Planet. Sci. Lett., 28, 459-469.

Yoder, H.S. and C.E. Tilley, 1962. Origin of basalt magmas: an experimental study of natural and synthetic rock systems, J. Petrol., 3, 342-532.

## APPENDIX

### PETROGRAPHIC DESCRIPTIONS

#### INTRODUCTION

Because chemical features of plutonic rocks are dependent on formation mechanisms, full petrographic descriptions are provided to aid evaluation of various chemical features. Descriptive textural terms are used and where relevant, "cumulus" terminology is also used in the sense discussed in chapter 2. Due to layering of some samples, thin section descriptions may not be entirely representative of the whole sample. Textures, modal proportions, and alteration are observed to vary somewhat among different thin sections cut from a single sample.

In addition to petrographic descriptions, other salient features which aid sample description are mentioned. These include semi-quantitative chemical observations (e.g., zonation, mineral identification) determined by electron microprobe, and brief description of outcrop relationships where helpful.

Generalized petrography of NAM plutonic rocks in this suite

Samples were chosen for this study on the basis of freshness. Degree of metamorphic alteration is greatest in the upper gabbros, and therefore most samples studied are from the lower isotropic gabbro and layered units and are mesocumulus or adcumulus textured. Orthocumulus textured rocks are represented only by sample 123. Because of the similarity among most of the mesocumulus and adcumulus textured rocks, a general description is useful.

The major primary minerals of these rocks are generally plagioclase, clinopyroxene, and olivine. Brown hornblende is prominent only in sample 777, and orthopyroxene only in sample 909. Each of the three major minerals may be included in any other. Each also appears as "interprecipitate" crystals, i.e., as small crystals located between the margins of other major crystals. Olivine and clinopyroxene especially occur at plagioclase triple junctions in gabbros. Because of these relationships, it is often not possible to establish a crystallization order from rock texture, but in fact these relationships are suggestive of co-precipitation.

Brown hornblende, orthopyroxene, and occasionally opaque oxides are usually minor and texturally appear interstitial to or in reaction relation with the major phases. Orthopyroxene partly rims and embays olivine and brown hornblende often partly rims clinopyroxene. The fact that they do not completely rim the major phases is suggestive that they crystallized from trapped pore liquid.

#### Plagioclase

Usually anhedral, except where included in olivine or clinopyroxene, where it sometimes is subhedral. Grain size range may be small in some samples and fairly large in others. It usually occurs as almost a monominerallic matrix (>50%) in gabbros, with variable amounts of interstitial ferromagnesian material. Optical zoning is normal and often present, but complete extinction usually occurs within  $10^{\circ}$  in most crystals. Zoning may be obscured by undulose extinction in some rocks. Most plagioclase is quite fresh but is somewhat clouded

(probably saussiterization) in a few samples, especially in cores. The amount and types of twinning is variable. Twin lamellae are sometimes bent and sometimes only partially penetrate the grains, suggesting at least some are strain induced. A few samples show mild sub-parallel alignment of lamellae.

#### Clinopyroxene

Clinopyroxene has three modes of occurrence; as equant anhedral crystals similar in size to other major phases, as small interstitial crystals, and as fairly large megacrysts, some of which are oikocrystic. The clinopyroxene is sometimes mildly optically zoned, especially the larger crystals. Some, especially the megacrysts, display prominent parting. Clinopyroxene generally occurs in clusters which are often elongated within the layering plane. It is often partly rimmed by brown hornblende and sometimes shows incipient alteration to brown hornblende. It is usually fairly fresh, but may show varying degrees of alteration to opaque oxide, chlorite, and fibrous amphibole. A few grains have prominent cleavage or parting controlled inclusions of opaque oxide in amounts considered too great to be exolved. Exolved opx is rarely seen.

#### Olivine

Olivine usually occurs in clusters of several anhedral crystals. These crystals are sometimes partly mantled by other olivine. These patches are often irregularly shaped and may extend as thin stringers between other major phases, giving the impression of being both a primary and an interstitial phase. Olivine also occurs as small

grains interstitial to clinopyroxene and plagioclase. Olivine patches are sometimes partially rimmed or embayed by small amounts of orthopyroxene. Alteration may range from very fresh to completely altered within a single sample. Common alteration products are magnetite, serpentine, and chlorite, with lesser talc, iddingsite, and bowlingite.

#### Brown hornblende

This is usually a minor interstitial phase or a replacement of clinopyroxene. It sometimes surrounds patches of opaque oxide.

#### Orthopyroxene

Orthopyroxene is usually a minor interstitial phase or a reaction replacement of olivine. A few crystals have small olivine cores.

#### Opaque oxides

These are presumedly mostly iron or iron-titanium oxides. It occasionally appears as a minor primary interstitial phase, occurring as anhedral masses. A few rare octahedra have been observed in plagioclase. The opaques are mostly an alteration product in olivine cracks and as blebs in clinopyroxene.

TABLE A-I

## MODAL MINERALOGY

SAMPLE	635A	709A	733B	800A	909A	910B	963A
PLAG	70.3	74.7	63.2	68.8	1.6	56.4	50.0
PYX (total)	2.0	18.7	30.9	17.0	81.7	36.0	32.7
CPX	~ 2.0	18.7	~ 30.9	~ 17.0	63.0 <sup>a</sup>	~ 36.0	32.7
OPX					19.0 <sup>a</sup>		
OLIV	26.6	4.7	5.4	10.0	16.0	7.2	7.3
Brown HB				1.5		0.4	3.9
OXIDES				0.3	0.4		2.7 <sup>b</sup>
OTHER <sup>c</sup>	1.1	1.8	0.5	2.4	0.4	0.2	3.4
TOTAL	100.0	99.9	100.0	100.0	100.0	100.0	100.0
# points	1093	1032	1067	1025	776	992	1109

a Calculated from whole-rock and mineral CaO analyses.

b Includes magnetite alteration product in olivine cracks.

c Includes all alteration products that couldn't be related to original igneous minerals.

Note: Clinopyroxene modes designated ~ in samples with minor but undetermined amounts of orthopyroxene.

TABLE A-II

## COMPARATIVE PETROGRAPHY

SAMPLE	ROCK TYPE	TEXTURE	CUMULATE CLASS	MAJOR PRIMARY MINERALS				ALTERATION
				PL	CPX	OL	OTHER	
HYPABYSSAL-EXTRUSIVE CARAPACE								
104C	pillow basalt	ophitic	--	X	X			mod
109C	diabase	subophitic	--	X	X			mod
ISOTROPIC GABBRO UNIT								
101C	trondhjemite	hypid. gran.	--	X	X		Qz	mod
102A	ol. gabbro	poik. hypid.	H	X	X	X		mod
123B	ferrogabbro	hypid.	O	X	X		Ox	mod
139A	gabbro	xen. gran.		X	X			ext
205C	ol. gabbro	poik. xen. gran.	A	X	X	X		min
630A	ol. gabbro	xen.	M	X	X	X		mod
633B	metagabbro	xen. gran.		X	X			ext
979B	ol. gabbro	xen. gran.		X	X	X		min



TABLE A-II (continued)

SAMPLE	ROCK TYPE	TEXTURE	CUMULATE CLASS	PRIMARY MINERALS			ALTERATION
				PL	CPX	OL OTHER	
LAYERED GABBROIC AND TRANSITION ZONE ROCKS							
308A	ol. gabbro	xen. gran.	A	X	X	X	min
635A	troctolite	xen. gran.	A	X		X	min
709A	ol. gabbro	xen.	A	X	X	X	min
720A	ol. gabbro	xen. gran.	A-M	X	X	X	mod
733B	ol. gabbro	xen. gran.	A-M	X	X	X	min
764C	ol. gabbro	xen.		X	X	X	min
777A	ol.-hb. gabbro	xen. gran.	A-M	X	X	X Hb	min
800A	ol. gabbro	xen. gran.	M	X	X	X	min
905A	wehrlite	cataclastic			X	X	mod
909A	lherzolite	xen. gran.	A		X	X Opx	min
910B	ol. gabbro	xen. gran.	A	X	X	X	min
963A	ol. gabbro	xen.	M	X	X	X	min

Notes: Textural terms: hypid.- hypidiomorphic; poik.- poikilitic; xen.- xenomorphic; gran.- granular.

Cumulus classes: A- adcumulus; O- orthocumulus; M- mesocumulus; H- heteradcumulus.

Alteration: min- fresh or minor; mod- moderate; ext- extensive, This is a relative classification, none of these samples are extremely altered.

Samples 905, 909, and 910 are from the transition zone.

## KEY

Sample number

Rock name

Lithologic unit (with supplemental description, where necessary)

Texture (descriptive, with modifying "cumulus type")

List of major "primocryst"

minerals (those that are present in significant amounts of about 5% or more, and which texturally appear to have been able to crystallize at the same time as the other major minerals). Modes are given, where determined, and also are listed in table A-1. Visual estimates of abundance are in parentheses.

List of minor, accessory, and

alteration minerals (those that appear to have crystallized only in the last stages of solidification; e.g., as rims on primary minerals or as small grains interstitial to primary crystals; or accessory minerals of minor elements, e.g., apatite; or alteration products of original minerals).

Description of major and important minor minerals, including habit, mineral relationships, significant optical properties (e.g., zoning), and alteration.

Comments - Description of any salient or unusual features, including comments about electron microprobe data.

101C

trondhjemite

Lithologic unit- dike cutting isotropic gabbro

Texture - hypidiomorphic granular

Major primary minerals

Minor, accessory, alteration minerals

plagioclase (albite)

opaque oxides

quartz

apatite

clinopyroxene

amphibole

chlorite

sphene?

Description

plagioclase - blocky subhedral crystals; very dusky, especially  
the cores; zoned; mostly Carlsbad twins

quartz - anhedral, equant crystals; prominent undulose  
extinction

clinopyroxene - mostly altered to amphibole, chlorite, and  
opaque oxides

102A

olivine gabbro

Lithologic unit - isotropic gabbro

Texture - poikilitic hypidiomorphic heteradcumulate

Major primary minerals

Minor, accessory, alteration minerals

plagioclase ( 70%)

chlorite

clinopyroxene ( 15%)

talc

olivine (15%)

opaque oxides

bowlingite?

Description

plagioclase - subhedral, lath shaped crystals; moderately optically zoned; twinned

clinopyroxene - anhedral; mostly large, optically continuous oikocrysts enclosing plagioclase and altered green pseudomorphs of olivine; oikocrysts extend between close plagioclases and appears interstitial

olivine - scarce fresh cores; altered partly or wholly to talc, chlorite, and magnetite; also pseudomorphed by green mineral (bowlingite?)

104C

basalt

Lithologic unit - pillow lavas

Texture - ophitic

Major primary minerals

Minor, accessory, alteration minerals

plagioclase

chlorite

clinopyroxene

opaque oxides

Description

plagioclase - a few rare microphenocrysts which are normally zoned; groundmass crystals are lath-shaped and rather cloudy

clinopyroxene - some fairly fresh, some quite altered; one euhedral crystal is located within a patch of chlorite

Comments

Chlorite is prominently scattered throughout, but several large patches occur. These may have been sites of olivine phenocrysts, but no textural evidence is present. Opaque oxides occur in prominent patches.

109C

diabase

Lithologic unit - 4 ft. thick dike intruding pillow lava

Texture - subophitic cumulophyric

Major primary minerals

Minor, accessory, alteration minerals

plagioclase

chlorite

clinopyroxene

opaque oxide

fibrous amphibole (actinolite?)

#### Description

plagioclase - occurs as both phenocrysts and mesostasis mineral; phenocrysts are in clusters of 2-6 crystals; phenocrysts are normally zoned, and more blocky than groundmass laths; all are euhedral-subhedral, and rather dusky; Carlsbad twins are common in the groundmass laths

clinopyroxene - generally anhedral; relatively fresh; at least one fairly large patch is optically continuous and partially encloses several plagioclase laths; the central region of this patch is altered to a green amphibole and chlorite

#### Comments

Chlorite ± fibrous amphibole is scattered throughout. A few fairly large patches of chlorite, about the size of plagioclase phenocrysts, may have been olivine phenocrysts, but no pseudomorphic texture is

evident. Small irregular opaque oxide patches are scattered throughout, mostly with chlorite, but occasionally it occurs surrounded only by plagioclase laths. Visual estimate of plagioclase phenocryst volume is no more than 3%. Thin section is cut by a thin vein of calcite (0.5mm).

205C

olivine gabbro

Lithologic unit - isotropic gabbro

Texture - xenomorphic-poikilitic adcumulate

Major primary minerals	Minor, accessory, alteration minerals
plagioclase	brown hornblende
clinopyroxene	
olivine	

## Description

plagioclase - monomineralic adcumulus patches with variable grain size; also, subhedral laths poikilitically enclosed by large cpx oikocrysts; optical zoning not certain - obscured by undulose extinction; grain size is smaller between large cpx grains - maybe crushed or recrystallized

clinopyroxene - mostly large oikocrysts enclosing plagioclase and olivine crystals; some oikocrysts have diagenous parting in center of grains, but generally missing in rims; some clusters of smaller anhedral grains; some large oikocrysts show mild optical zoning, verified by microprobe

Olivine - very large irregular patches, often occurring partly rimming and rimmed by cpx; also, discrete grains enclosed by cpx oikocrysts; mildly undulose and possibly zoned; variably altered to iddingsite,



serpentine, talc, and magnetite

brown hornblende - interstitial and partly rimming cpx

#### Comments

The slight zoning of cpx oikocrysts suggests heteradcumulus growth, while the moderate amount of interstitial brown hornblende supports a mesocumulus classification. A qualitative microprobe traverse across one cpx oikocrysts confirms the moderate normal chemical zoning.

The rock is somewhat fractured and olivine extinction is undulose in some grains. Microprobe traverses across an olivine and a plagioclase crystal enclosed in a cpx oikocryst showed minor normal zoning.

123B

ferrogabbro

Lithologic unit - isotropic gabbro

Texture - hypidiomorphic granular orthocumulate

Major primary minerals	Minor, accessory, alteration minerals
plagioclase	amphiboles
clinopyroxene	chlorite
opaque oxides	opaque oxides

## Description

plagioclase - interlocking subhedral laths and blocky crystals;  
 moderate normal zoning; moderately to highly  
 sausseritized

clinopyroxene - anhedral patches interstitial to plagioclase; most  
 is rather highly altered to brown and green  
 amphiboles, especially on rims; some has a dusky  
 appearance with fine blebs of opaque oxide scattered  
 throughout

opaque oxides - occur as large anhedral patches both interstitial  
 to and poikilitically enclosing plagioclase crystals

amphiboles - both brown hornblende and green amphibole are present;  
 most is an alteration product, especially of  
 pyroxene, but some may be a later primary magmatic  
 phase; some is an acicular blue-green to pale green  
 pleochroic variety

### Comments

Olivine may have originally been present, but this is not certain. A few patches of chlorite and opaque oxide is vaguely suggestive of olivine texture.

139A

Gabbro

Lithologic unit - isotropic gabbro

Texture - xenomorphic granular

## Major primary minerals

plagioclase

clinopyroxene

## Minor, accessory, alteration minerals

chlorite

amphibole (actinolite?)

talc

opaque oxides

brown hornblende

green hornblende

sericite

## Description

plagioclase - anhedral, equigranular, moderately twinned; some optical zoning; patchy alteration to sericite and possibly sausserite; contains some small high relief inclusions, probably clinopyroxene

clinopyroxene - anhedral; equant; some poikilitic enclosure of plagioclase; cloudy, most shows at least partial alteration to green and brown hornblende, and possibly chlorite

## Comments

Alteration is extensive. One patch of talc and magnetite has possible olivine relict texture. One hornblende grades from green to

brown. A few muscovite crystals are large enough for positive identification.

308A

olivine gabbro

Lithologic unit - layered gabbro

Texture - xenomorphic granular adcumulate

Major primary minerals

Minor, accessory, alteration minerals

plagioclase

orthopyroxene

clinopyroxene

brown hornblende

olivine

green amphibole

## Description

plagioclase - anhedral, equant crystals; no apparent zoning; looks interstitial in clinopyroxene rich layers

clinopyroxene - mostly equant, anhedral grains; one shows incipient alteration to pale green amphibole; one large crystal encloses a smaller cpx and subhedral plagioclase; some have many high relief inclusions

olivine - varies from fairly fresh to largely altered to serpentine and opaque oxides; anhedral, occurring in patches; also occurs as interstitial phase

Orthopyroxene - may be fairly prevalent; some occurs as reaction product of olivine; a few larger, distinct grains with good cleavage are present; one subhedral grain **has** olivine core; may also occur as high relief, clear grains interstitial to clinopyroxene, but this is not verified

## Comments

This rock is layered, with alternating plagioclase rich or clinopyroxene rich bands. It shows good adcumulus texture.

630A

olivine gabbro

Lithologic unit - isotropic gabbro

Texture - xenomorphic mesocumulate

## Major primary minerals

plagioclase ( 70%)  
 clinopyroxene (25% total pyx.)  
 olivine (3-4%)

## Minor, accessory, alteration minerals

bronzite  
 brown hornblende  
 iddingsite  
 green amphibole

## Description

plagioclase - grain size varies considerably; significant strain induced twinning; rounded, anhedral grains with dusky cores and thin, clear rims; a few grains show minor optical zoning; a few rounded grains are included in the large cpx

clinopyroxene - quite fresh; occurs as fairly large anhedral grains, occasionally including both olivine and plagioclase; also as smaller discrete anhedral grains, usually associated with and partially rimming olivine; some large grains show moderate zoning; a few small grains at plagioclase triple junctions

olivine - as irregular patches of anhedral grains, often rimmed by cpx and opx; also appears, with or without cpx,



as stringers and small patches interstitial to plagioclase; mostly quite fresh, but in places is completely altered to opaques and iddingsite (verified by microprobe), but retain the typical olivine texture; the altered patches follow fractures; one grain partially enclosed by cpx has a rim of olivine of different optical character (birefringence, extinction) and 0.5 % Fo lower, and is subhedral; this grain is embayed by opx where not surrounded by cpx

orthopyroxene - small grains rimming olivine

brown hornblende - interstitial to and partly rimming cpx; also within margins of some cpx

633B

metagabbro

Lithologic unit - isotropic gabbro

Texture - xenomorphic granular

Major primary minerals	Minor, accessory, alteration minerals
plagioclase (50%)	bluish-green amphibole
clinopyroxene (25%)	chlorite
	hematite

## Description

plagioclase - mostly anhedral; slightly dusky; many twins, some bent, indicating strain; undulose extinction; moderate optical zoning; a few subhedral grains partially enclosed in cpx

clinopyroxene - rather dusky; in places riddled with opaque patches and/or parting controlled inclusions; at least one crystal has a patch of blue-green amphibole in its core and probably shows incipient alteration to the amphibole

## Comments

This is the most highly altered plutonic rock in this suite. Plagioclase is slightly dusky. At least 25% of this rock consists of patches of mainly chlorite and amphibole, some of which is due to alteration of clinopyroxene. No textural evidence of the former presence of olivine is present, but the amount of alteration products

and the fairly well preserved nature of much of the pyroxene suggest some of the chlorite and amphibole may be from alteration of olivine. The ferromagnesian alteration products occur also in fractures and between plagioclase grains. Some of the larger amphiboles have a pale yellow or colorless core with blue-green margins and may be actinolite and ferroactinolite or blue-green hornblende.

635A

clinopyroxene troctolite

Lithologic unit - layered gabbro

Texture - xenomorphic granular adcumulate

Major primary minerals

Minor, accessory, alteration minerals

plagioclase (70.3%)

clinopyroxene (2.0%)

olivine (26.6%)

brown hornblende

## Description

plagioclase - anhedral; occurs mostly as monomineralic matrix with few interstitial ferromagnesian minerals; occasionally included in olivine patches; quite fresh, with only minor alteration material between grains and in cracks; some undulose extinction; v. minor zoning

Olivine - clusters of anhedral crystals; patches extend between plagioclase grains in thin stringers and appear to surround and fill spaces between plagioclase crystals; some large, irregular, optically continuous olivines; a thin corona of isotropic material (perhaps hydrogarnet) surrounds most olivine patches bordering plagioclase, but is lacking between individual olivines; larger grains around olivine have been identified as clinopyroxene by microprobe, but some may be orthopyroxene, because most has quite low birefringence, and at least 1 grain with a diffuse margin on olivine has parallel extinction

and a tiny core of highly birefringent material (ol?); cpx rim on the same olivine patch nearby; very slight zoning is sometimes seen, and some grains are slightly undulose; olivine is quite fresh but highly fractured, with only minor alteration to magnetite in cracks

clinopyroxene - mostly as thin partial rims on olivine patches, but some of the grains are as large as individual olivines; occasional isolated crystals or small clusters wholly segregated from olivine; much of the thin pyroxene corona has low birefringence (first order gray) but a few probed points indicate clinopyroxene; orthopyroxene is not positively identified but is probable in very small amount

709A

olivine gabbro

Lithologic unit - layered gabbro

Texture - xenomorphic adcumulate

Major primary minerals

Minor, accessory, alteration minerals

plagioclase (74.7%)

brown hornblende

olivine (4.7%)

opaques

clinopyroxene (18.7%)

## Description

plagioclase - medium sized, anhedral, equant crystals with extensive twinning; 75% of rock is monomineralic sea of plagioclase; a few crystals enclosed in large cpx crystals; slightly to moderately clouded (sausserite?) twins have vague planar preferred orientation and many are bent; minor optical zoning in some grains

olivine - irregular patches of anhedral grains; some glassy fresh, some almost completely altered to opaques and serpentine ; highly fractured

clinopyroxene - mostly large anhedral, equant crystals, often with smaller crystals around the margins; pronounced parting or cleavage in megacrysts; a very few small crystals are interstitial to plagioclases

## Comments

Rock has moderate amount of brittle fractures, with most of the alteration located near these fractures. There are very few ferromag-

nesian crystals interstitial to plagioclases, consistent with the calculated low pore volume ( 11%). Optical zoning of plagioclase is not evident, but clouding and fracturing may obscure it. However, microprobe analyses show constant Ca<sup>#</sup> (75) for five widely separated crystals. These observations are consistent with an "adcumulus" classification.

720A

olivine gabbro

Lithologic unit - layered gabbro

Texture - xenomorphic granular

## Major primary minerals

## Minor, accessory, alteration minerals

plagioclase

brown hornblende

clinopyroxene

orthopyroxene

olivine

talc

magnetite

bowlingite

## Description

plagioclase - anhedral, equant crystals; fairly fresh; many are separated by hydrous ferromagnesian material which appears to have come from altered olivine and migrated between the plagioclase crystals; slight to moderate zoning

clinopyroxene - equant, anhedral crystals; generally occur in clusters or bands; some have anhedral blebs of opaque oxide; some have tiny, cleavage controlled inclusions, possibly opx exolution features

olivine - some moderately fresh cores; occur mostly in patches; rims generally corroded to talc and magnetite; some patches completely altered; an isotropic material often rims these patches where in contact with plagioclase (hydrogarnet?); some altered to



## bowlingite

brown hornblende - mostly within and between clinopyroxenes; a few small isolated grains; mostly anhedral, a few subhedral

orthopyroxene - small anhedral crystals with clinopyroxene and between plagioclases; one has small olivine core

opaque oxides - mostly irregular blebs in clinopyroxene, but two euhedral octahedra are included in a plagioclase

## Comments

Rock is moderately altered. Most individual plagioclases have been spread apart by hydration and migration of hydrous ferromagnesian material. This makes it difficult to estimate the amount of pore material.

733B

olivine gabbro

Lithologic unit - layered gabbro

Texture - xenomorphic granular

## Major primary minerals

plagioclase (63.2%)

clinopyroxene (30.9% total pyx)

olivine (5.4%)

## Minor, accessory, alteration minerals

orthopyroxene?

opaques

brown hornblende

iddingsite

bowlingite

## Description

plagioclase - fresh, anhedral crystals; some undulose; unzoned; monomineralic matrix with very little interstitial material, but occasional small interstitial cpx

clinopyroxene - medium to large anhedral crystals, some with prominent parting, often surrounded by smaller equant anhedral crystals; also as small grains at plagioclase triple junctions; some olivine patches are rimmed by cpx; two crystals are distinctly zoned, but most are not

olivine - anhedral crystals in patches; some patches rimmed by cpx (and possibly opx) while others are not; alteration is quite variable, ranging from glassy fresh to strongly altered to iddingsite, opaques and serpentine, and probably bowlingite

751A

olivine gabbro

Lithologic unit - layered gabbro

Texture - xenomorphic granular mesocumulate

Major primary minerals

Minor, accessory, alteration minerals

plagioclase

brown hornblende

clinopyroxene

orthopyroxene

olivine

Description

plagioclase - equant, anhedral; a few grains enclosed in cpx are subhedral; moderate twinning; sharp extinction, zoning not evident

clinopyroxene - occurs in two distinct modes; one as very large anhedral grains with prominent parting (diallage?); these large grains enclose subhedral plagioclase crystals; cpx also occur as smaller grains which in places appears interstitial to plagioclase

olivine - anhedral; in patches; much is badly fractured, with alteration to opaques and serpentine; occurs both with cpx and in cpx free patches; very small rounded grains enclosed by plagioclase may be olivine; occurs in small patches at plagioclase triple junctions

orthopyroxene - very minor; very thin partial rim on one olivine patch, with first order gray birefringence and parallel extinction; other small grains are

suspected as orthopyroxene

brown hornblende - mostly small crystals interstitial to clinopyroxene and as thin rims between cpx and plagioclase; a few grains are nearly as large as medium sized clinopyroxenes; two rimming olivine have parallel extinction

#### Comments

Rock is banded, with bands being vague and defined by proportion of olivine: clinopyroxene. The cpx rich layer has significant brown hornblende. The rock is also rather fractured, with the greatest concentration of cracks in and near olivine, and roughly parallel to banding. Olivine, cpx, and hornblende all occur as small crystals at plagioclase triple junctions, and this rock has a large amount of this material, consistent with a calculated high amount of trapped pore liquid ( 18%).

777A

olivine-hornblende gabbro

Lithologic unit - layered gabbro

Texture - xenomorphic granular adcumulate

Major primary minerals	Minor, accessory, alteration minerals
plagioclase	apatite
clinopyroxene	opaque oxides
olivine	Fe-Ti sulfide
brown hornblende	

## Description

plagioclase - anhedral, equant, moderately twinned; has inclusions of cpx, hb, titanomagnetite; occurs as small rounded (partially resorbed?) inclusions in clinopyroxene, hornblende

clinopyroxene - anhedral, fairly equant grains; occur more as individual crystals or clusters of a few crystals rather than large clusters like most other samples; also as small subrounded to euhedral inclusions in plagioclase; has a purplish tinge

olivine - occurs as anhedral crystals in large patches in one half of thin section and as rarer, individual or small clusters of crystals on the other half; the smaller crystals especially have opaque oxide corroded margins rather than within cracks like most other samples (maybe due to high fayalite content); also

occurs as small inclusions in brown hornblende  
 brown hornblende - abundant major phase; anhedral equant crystals  
 appear primary; also as small euhedral to rounded  
 inclusions in plagioclase and clinopyroxene; semi-  
 quantitative microprobe analyses show significant  
 $\text{TiO}_2$  content, and similar compositions for both modes  
 of occurrence

other - needle or rod shaped apatite inclusions in plagioclase;  
 titanomagnetite octahedra included in plagioclase  
 and Hb; one small patch of Fe-Ti sulfide identified

#### Comments

This rock is unusual in texture, mineralogy, and chemistry.  
 Texturally, it is finer grained (avg. diameter 0.2 mm) than most other  
 plutonic rocks of NAM. The major minerals are all equant and similar  
 in size. Also many combinations of minerals are included in one  
 another. Abundant primary hornblende is also unusual. Chemically, this  
 rock has unusually high incompatible element concentrations, and highly  
 evolved olivine ( $\text{Fo}_{62}$ ) and plagioclase ( $\text{Ca}^\# = 60$ ).

Extensive microprobe analysis of this slide has shown the included  
 cpx and hb have compositions similar to the larger primary crystals.  
 Semi-quantitative microprobe analyses were used to verify mineral  
 identification.

800A

olivine gabbro

Lithologic unit - layered gabbro

Texture - xenomorphic granular mesocumulate

## Major primary minerals

## Minor, accessory, alteration minerals

plagioclase (68.8%)

brown hornblende (1.5%)

clinopyroxene (17.0% total pyx)

orthopyroxene

olivine (10.0%)

opaque oxides

hematite

apatite

## Description

plagioclase - equant, anhedral; minor zoning; very fresh; include small olivines and clinopyroxenes; one fairly large apatite inclusion observed; a few small subhedral crystals included in clinopyroxene

clinopyroxene - mostly equant, anhedral crystals; often clustered in bands; a few larger megacrysts ( 3 times average diameter) occur; also as small crystals interstitial to plagioclase; slight optical zoning, especially in larger crystals

olivine - generally very fresh, with magnetite in cracks; occurs as small clusters of irregularly shaped, optically continuous crystals; also as equant anhedral grains; also as small crystals interstitial to plagioclase

brown hornblende - more than in most layered gabbros; usually within  
and between clinopyroxenes, occasionally partly rimming  
cpx; a few free crystals with cleavage developed  
orthopyroxene - minor; embays and partly rims some olivines  
opaque oxides - generally anhedral; occurs as irregular blebs in  
clinopyroxenes, as irregular patches between major  
primocrysts, and as an alteration product in olivine  
cracks

#### Comments

This sample is very fresh. Fine scale banding is defined by both grain size variation and modal proportions. Some of the opaque oxide is probably a primary phase. The abundant oxide and hornblende, as well as interstitial olivine and clinopyroxene, suggest a fair amount of trapped liquid. The estimated amount, based on Zr, is about 15%. Microprobe analyses of a megacryst show moderate normal zoning.



905A

wehrlite

Lithologic unit - transition zone

Texture - cataclastic, mylonitic

Major primary minerals

clinopyroxene (70-80%)

olivine (20-30%)

Description and Comments

Both olivine and clinopyroxene are fairly fresh looking but are granulated. The minerals tend to be segregated into layers. Grain size is fairly small, due partly to crushing texture. The rock is highly deformed, and is cut by several subparallel mylonite zones in two directions.

909A

lherzolite

Lithologic unit - transition zone

Texture - xenomorphic granular adcumulate

Major primary minerals	Minor, accessory, alteration minerals
clinopyroxene	plagioclase (1.6%)
orthopyroxene	opaques
olivine (16.0%)	
(total pyroxene 81.7%)	

## Description

clinopyroxene - medium sized anhedral crystals in clusters; bounds both olivine and opx

olivine - glassy fresh, anhedral grains in patches; often surrounded and partly embayed by opx; patches form an unusual net-like texture surrounding patches of pyroxene; some mildly undulose; cracks filled with magnetite and serpentine

orthopyroxene - anhedral; occurs as distinct crystals completely bounded by cpx or other opx; also occurs partly embaying olivine; glassy with very faint pink-colorless pleochroism

plagioclase - occurs a two very small clusters and a few rare small isolated grains, clearly interstitial to the ferro-magnesian phases

## Comments

This rock is the most unusual in terms of mineral assemblage. Unlike all other plutonic samples, with the possible exception of #308, orthopyroxene appears to be a primary phase, crystallizing before plagioclase. In all other samples, it appeared as a late reaction phase on olivine, crystallizing after plagioclase. The texture and mineralogy of this sample suggest the liquid was on the  $\text{cpx} + \text{ol} + \text{opx}$  cotectic/reaction boundary before reaching the quaternary pseudoinvariant point. Only one other sample from the Bay of Islands layered rocks is reported to contain primary orthopyroxene, a gabbro reported by Church and Riccio (1977).

910B

olivine gabbro

Lithologic unit - transition zone

Texture - xenomorphic granular adcumulate

Major primary minerals

Minor, accessory, alteration minerals

plagioclase (56.3%)

brown hornblende (0.4%)

clinopyroxene (36.0% total pyx)

orthopyroxene

olivine (7.2%)

Description

plagioclase - mostly equigranular, anhedral crystals; some undulose extinction; very slight edge zoning in some crystals; fairly minor amount of twinning, mostly Carlsbad with some albite or pericline; some twins show only partial penetration; very fresh; one small subhedral lath is enclosed in a patch of olivines

olivine - generally small anhedral crystals, always associated with pyroxene; often appears at the margins of pyroxenes, almost rim-like, and also between clinopyroxene crystals; quite fresh, with minor magnetite in cracks

clinopyroxene - anhedral crystals, at least one simply twinned; slight zoning in a few crystals; most about the same size as plagioclase, but a few small grains occur at plagioclase triple junctions

orthopyroxene - clear, glassy, anhedral crystals; one has small olivine remnant in core

brown hornblende - very thin partial rim on some clinopyroxenes

#### Comments

This sample is one of the best examples of adcumulus texture in this suite. It is also one of the least altered. Modal pyroxene is 36%, and calculations based on whole rock and mineral CaO compositions indicate about 3-5% of it is opx, assuming average  $\text{CaO}_{\text{opx}}$  1-1.5% and the amount of CaO in hornblende (mode = 0.4%) is negligible.

963A

olivine gabbro

Lithologic unit - layered gabbro

Texture - xenomorphic mesocumulate

Major primary minerals

Minor, accessory, alteration minerals

plagioclase (50.0%)

brown hornblende (3.9%)

clinopyroxene (32.7%)

opaque oxide

olivine (7.3%)

Description

plagioclase - anhedral; fairly fine grained; slight to moderate zoning; markedly twinned; in some patches, lacking any noticeable interstitial ferromagnesian phase, but elsewhere (especially where olivine is the main ferromagnesian phase) there is a fair amount of small cpx and olivine and a little opaque oxide in the interstices

clinopyroxene - anhedral, blocky; occurs mostly in patches of medium sized grains, often with significant interstitial hornblende and opaques; a few large grains are present, a few of which are twinned, and enclose some smaller cpx grains; also as very small grains interstitial to plagioclase; also partially rims olivine patches; moderate zoning

olivine - occurs mainly as clusters of anhedral grains; appears the main ferromagnesian phase in one layer and also as

small grains interstitial to plag in this layer; elsewhere it is secondary in abundance to cpx; mostly fresh but some alteration to serpentine and opaques, and iddingsite other - brown hornblende and opaque oxide occurs mainly interstitial to clinopyroxene and in a few places, plagioclase, oxide also is a prominent exsolution? feature in some clinopyroxenes

#### Comments

Olivine and clinopyroxene appear to be both primary ferromagnesian phase and a pore component interstitial to plagioclase, suggesting the three phases were co-saturated. The significant amount of hornblende and oxides interstitial to clinopyroxene, and of cpx and olivine interstitial to plagioclase, suggest a mesocumulate texture. The prominent opaque exsolution in cpx may indicate re-crystallization.

Vague layering is seen in thin section defined by change in proportion between cpx and olivine, and also elongation of the ferromagnesian patches.

Rock is quite fresh but moderately fractured. Much of the alteration occurs along these fractures.

979B

olivine gabbro

Lithologic unit - isotropic gabbro

Texture - xenomorphic granular

Major primary minerals

Minor, accessory, alteration minerals

plagioclase (70%)

brown hornblende (1%)

clinopyroxene (18% total pyx)

opaque oxide

olivine (10%)

orthopyroxene

## Description

plagioclase - anhedral; some quite large with undulose extinction, others quite small; fresh; twins are crudely sub-parallel to banding defined by elongation of ferromagnesian patches; twins, especially in large crystals, are partial and bent; undulose extinction obscures any optical zoning, if present

clinopyroxene - clusters of anhedral crystals, often surrounding patches of olivine, but occasionally alone; rims olivine in places, along with opx; shows incipient change to brown hornblende; cleavage or parting controlled opaques included; some small grains in plagioclase interstices

olivine - mostly anhedral crystals in patches and stringers which look interstitial to plagioclase; a few equant subhedral crystals within patches; mostly fresh with minor alteration to serpentine and opaques; one



unusual teardrop shaped olivine with cpx rim on pointed end is partially included in a large, strained plagioclase crystal

hornblende - brown, anhedral crystals; fair amount, some between cpx crystals, some within the cpx suggesting alteration of cpx

orthopyroxene - partial rims on olivine, and discrete grains intimate with olivine; some orthopyroxene is surrounded by brown hornblende

#### Comments

Some unusual textural features suggest this rock may have undergone partial recrystallization. The large variation in plagioclase grain size and the highly strained nature of the larger grains (twin style, undulose extinction) and the inclusion of smaller plagioclase in larger grains suggest smaller grains have grown in replacement of larger ones.